Chem-85

Synthesis of Natural Products-Stabilized Nanoparticles and Their Potential Applications in Wound Dressings and Medical Diagnosis of Cysteine/Cystine Related Renal Diseases

CAI Gen
FUNG Tin-yau
ZHANG Jiacheng
LUI Bob, Head of Gifted Education Committee and Science Research Team
King's College, Hong Kong, China

2022 S.-T. Yau High School Science Award
仅用于2022丘成桐中学科学奖公示

2022 S.T. Yau High School Science Award (Asia)

Research Report

The Team

Registration Number: Chem-85

Name of team member: CAI Gen
School: King's College
City, Country: Hong Kong, China

Name of team member: FUNG Tin-yau
School: King's College
City, Country: Hong Kong, China

Name of team member: ZHANG Jiacheng
School: King's College
City, Country: Hong Kong, China

Name of supervising teacher: LUI Bob
Job Title: Head of Gifted Education Committee and Science Research Team
School: King's College
City, Country: Hong Kong, China

Title of Research Report

Synthesis of Natural Products-Stabilized Nanoparticles and Their Potential Applications in Wound Dressings and Medical Diagnosis of Cysteine/Cystine Related Renal Diseases

Date

31 August 2022

2022 S.T. Yau High School Science Award
仅用于2022丘成桐中学科学奖公示

Synthesis of Natural Products-Stabilized Nanoparticles and Their Potential Applications in Wound Dressings and Medical Diagnosis of Cysteine/Cystine Related Renal Diseases

CAI Gen, FUNG Tin-yau, ZHANG Jiacheng

1 Abstract

The aim of this project is to optimize the methodology of the preparation of natural products-stabilized metal nanoparticles, and to assess their antibacterial and antifungal properties, their application on the synthesis of hydrogels, and the detection of cysteine. In this project, silver nanoparticles (AgNPs) and copper nanoparticles (CuNPs) were synthesized in an eco-friendly way using different reducing agents and naturally-occurring capping agents. Current methodologies [1]make use of ready-made, and sometimes inorganic, chemicals as the capping and reducing agents of the nanoparticles. Apart from using these chemicals, our study also made use of various natural products, such as extracts of okra plants and avocado seeds, to synthesize Ag and CuNPs, such that they were more eco-friendly and more biocompatible [2–4].

Various parameters, namely the type of metal ion, the type and concentration of the capping agent and reducing agent, and the reaction temperature, were varied to produce different types of nanoparticles. Chitosan, alginate, okra mucilage and starch-chelated AgNPs were successfully synthesized with excellent stability. However, CuNPs were unstable and oxidized spontaneously. Potassium iodide was added to stabilize the CuNPs by forming impermeable CuI layers, but they were still oxidized and underwent a colour change from wine red to yellow within 24 hours at 4℃.

Successfully synthesized nanoparticles were tested for their antibacterial and antifungal properties. Starch-chelated AgNPs (Starch/AgNPs), alginate-chelated AgNPs (Alginate/AgNPs) and Chitosan-chelated AgNPs (Chitosan/AgNPs) were used to synthesize hydrogels. Multiple crosslinking mechanisms were proposed.

In our preliminary section, it was found that Chitosan/AgNPs, Starch/AgNPs and Alginate/AgNPs exhibited a significant antibacterial effect, with the minimum inhibitory concentration being 4.17 ppm, which was less than half of the commercial value [5]. Only at a high concentration, namely 100 ppm, could the nanoparticles exhibit a notable antifungal effect. Moreover, the nanoparticles were found to be able to crosslink with PVA to form hydrogels.

It is found that the interaction between AgNPs (conc. of 100 ppm) and cysteine ($C_3H_7NO_2S$) molecules resulted in a sharp, instant colour change at [Cysteine] ≥ 20 ppm. Furthermore, it is found that cystine, ($C_6H_{12}N_2O_4S_2$) did not exhibit the same result when interacting with AgNPs; however, a buffer containing SO_3^{2-} was developed for reducing cystine to cysteine, allowing the detection of cystine. This method could be used for screening several diseases relating to the abnormalities in the cysteine and cystine levels, such as cystinuria [6], hyperhomocysteinemia and other renal diseases [7].

2022 S.T. Yau High School Science Award 仅用于2022丘成桐中学科学奖公示

Keywords: silver nanoparticles, copper nanoparticles, okra, alginate, chitosan, starch, antibacterial, wound dressings, hydrogels, cysteine, cystine, cystinuria, hyperhomocysteinemia, renal diseases.

2 Acknowledgement

1. School chemistry and biology teachers, who provide professional comments and advice.
2. Laboratory technicians and laboratory attendants, who assisted us in preparative works in the senior chemistry laboratory.

2022 S.-T. Yau High School Science Award
仅用于2022丘成桐中学科学奖公示

3 Commitments on Academic Honesty and Integrity

We hereby declare that we

1. are fully committed to the principle of honesty, integrity and fair play throughout the competition.
2. actually perform the research work ourselves and thus truly understand the content of the work.
3. observe the common standard of academic integrity adopted by most journals and degree theses.
4. have declared all the assistance and contribution we have received from any personnel, agency, institution, etc. for the research work.
5. undertake to avoid getting in touch with assessment panel members in a way that may lead to direct or indirect conflict of interest.
6. undertake to avoid any interaction with assessment panel members that would undermine the neutrality of the panel member and fairness of the assessment process.
7. observe the safety regulations of the laboratory(ies) where the we conduct the experiment(s), if applicable.
8. observe all rules and regulations of the competition.
9. agree that the decision of YHSA(Asia) is final in all matters related to the competition.

We understand and agree that failure to honour the above commitments may lead to disqualification from the competition and/or removal of reward, if applicable; that any unethical deeds, if found, will be disclosed to the school principal of team member(s) and relevant parties if deemed necessary; and that the decision of YHSA(Asia) is final and no appeal will be accepted.

Name of team member: CAI Gen

Name of team member: FUNG Tin-yau

Name of team member: ZHANG Jiacheng

Name of supervising teacher: LUI Bob

Noted and endorsed by

(signature)

Name of school principal: WONG Chau-ling, Fiona

2022 S.T. Yau High School Science Award
仅用于2022丘成桐中学科学奖公示

Table of Contents

2022 S.-T. Yau High School Science Award
仅用于2022丘成桐中学科学奖公示

4 Introduction

AgNPs are receiving increasing attention from researchers due to their excellent antibacterial properties, which can be used in disinfecting open wounds on the skin. Furthermore, traditional antibiotics are ineffective against drug-resistant bacteria strains. The USA Centers for Disease Control and Prevention have predicted more deaths from antimicrobial-resistant bacteria than all types of cancers combined by 2050 [8]. Therefore, AgNPs, being a non-antibiotic-based material, can be used to resolve the problem. They have an especially high potential in treating burn and chronic wounds as their healing process are slow, and the chance of infections is high.

Among the various capping agents of AgNPs, natural polymers, such as chitin, alginate and starch, are desired because of their high biocompatibility [8]. AgNPs are also capable of being functionalized with hydrogels. A hydrogel is a three-dimensional, hydrophilic, crosslinked insoluble polymeric matrix with the ability to extend and retain a significant fraction of water within its structure. Hydrogels are usually synthesized by the crosslinking of hydrophilic polymers by the reaction

2022 S.-T. Yau High School Science Award
仅用于2022丘成桐中学科学奖公示

between functional groups and external chemicals. The AgNPs-hydrogel composite often features properties like high porosity, hydrophilicity, swelling capacity and lack of toxicity, which is desired in an ideal wound dressing [9].

K. K. Y. Wong *et al.* [10]also reported that the healing process of second-degree burn wounds was accelerated in BALB/C mice when they are treated with AgNPs. It has been shown that AgNPs can modulate the cytokines involved in the wound-healing process and give a better cosmetic appearance.

Currently, the exact mechanism of AgNPs' antibacterial effect is not completely understood, but there are several proposed mechanisms. AgNPs can physically penetrate the bacterial wall and membrane, leading to cell lysis [11], and interact with thiol-containing proteins.

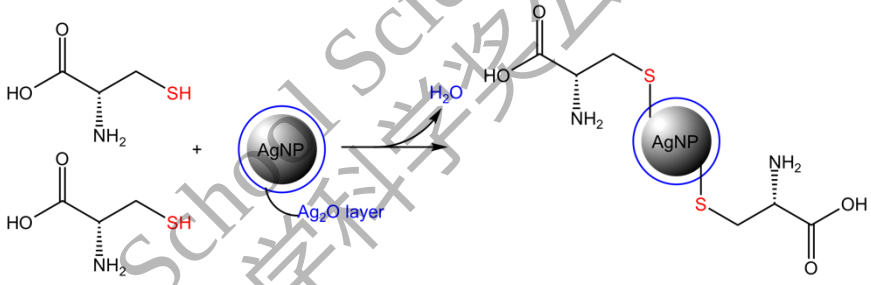

Equation 1: a demonstration of the interaction between AgNPs and thiol groups (in red colour) using L-cysteine as a model.

In addition, AgNPs can continuously release Ag^+ ions which kill bacteria. Ag^+ ions can destroy the cell wall and membrane by denaturing outer membrane structures, such as thiol-containing proteins [11,12]. This enhances the permeability of the cell membrane and causes bacteriolysis. Inside the cell, Ag^+ ions can react with the thiol groups (-SH) of proteins [13]and bind with their active sites, resulting in reduced enzymatic activities in the organism. For example, the thiol groups of glyceraldehyde-3-phosphate dehydrogenase (GAPDH), an important enzyme for glycolysis, and malate dehydrogenase (MDH), a key enzyme in the central oxidative pathway [14], were bonded to Ag^+ ions and this resulted in reduced activities [15]. The ions can initiate the generation of reactive oxygen species (ROS), such as O_2^-, •OH, and H_2O_2, causing oxidative stress [8,11,16]. Furthermore, ROSs can cause damage within DNA pairs, especially GC base pairs, interrupting cell replication and inhibiting the growth of the bacteria. The enzymes required in the repair of DNA, such as GAPDH [17], are also inhibited.

2022 S.-T. Yau High School Science Award
仅用于2022丘成桐中学科学奖公开

There are several advantages of using AgNPs over $AgNO_3$ and silver sulfadiazine, such as their extremely slow release of Ag^+ ions and them being less irritative [8]. More importantly, AgNPs have extremely low toxicity towards animals, with a median lethal dose (LD_{50}) of 250 – 350 mg/kg [18]. Nevertheless, there are still a lot of unknown impacts of AgNPs on human health [8].

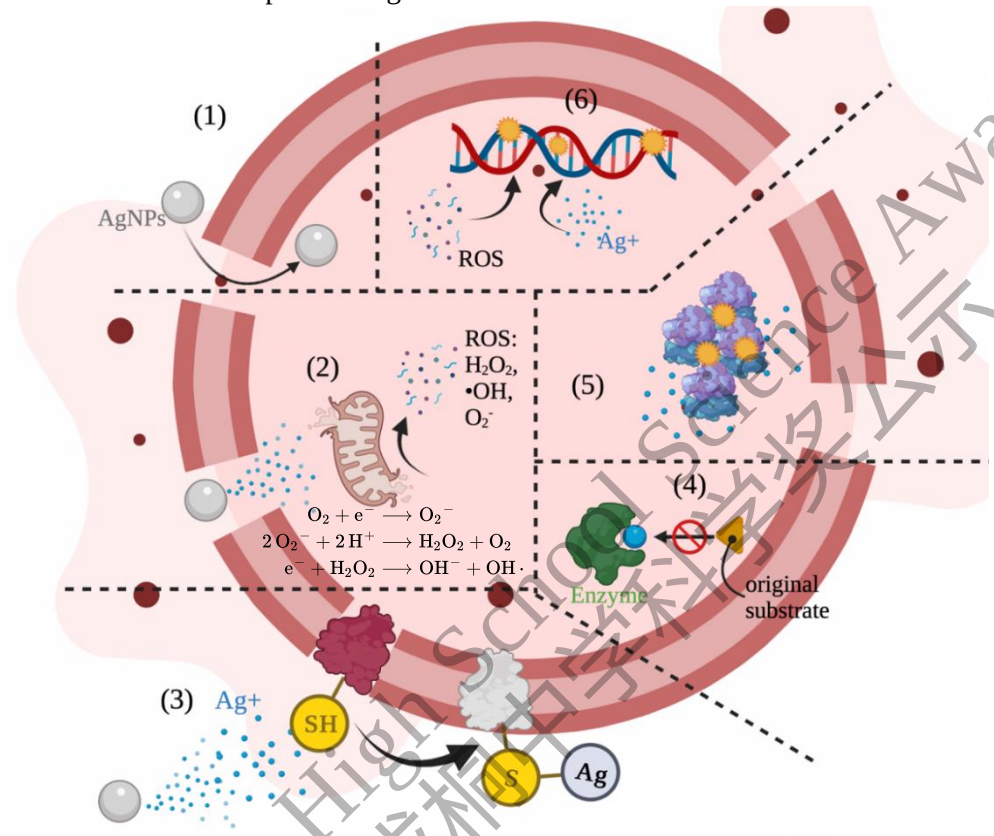

Figure 1: the antibacterial activities of AgNPs. (1) AgNPs perforate the bacteria cell wall, leading to bacteriolysis; (2) one possible route for generating ROSs, which involves Ag^+-caused mitochondrial dysfunction; (3) AgNPs and Ag^+ ions denature the membrane proteins by binding with the thiol group; (4) Ag^+ ions act as enzyme inhibitors by binding to the active site of enzymes; (5) Ag^+ ions denature ribosomes and inhibit protein synthesis; (6) Ag^+ ions and ROS cause DNA oxidation. Generated from BioRender

In this report, AgNPs were synthesized in a green way with different natural capping agents, and their antibacterial and antifungal properties were investigated. The approach to forming nanoparticle-hydrogel composite was brought by the gelation of the synthesized nanoparticles in hydrogel-forming polymers by crosslinking long polymer chains of PVA with mainly nanoparticles and a significantly low amount of borax.

2022 S.T.Yau High School Science Award
仅用于2022丘成桐中学生科学奖公示

5 Synthesis of nanoparticles

5.1 Experimental

5.1.1 Materials

The materials used for the synthesis of nanoparticles include silver nitrate, copper(II) chloride 2-hydrate, starch, sodium borohydride, L-ascorbic acid and potassium iodide (purchased from Uni-Chem), sodium alginate (purchased from Uni-Chem and Philip Harris), chitosan (purchased from J&K Scientific), cysteine (purchased from Alfa Aesar), acetic acid and ammonia solution (purchased from VWR Chemicals), pH10 buffer solution (purchased from Hanna Instruments), sodium hydroxide (purchased from Fisher Scientific), glucose (purchased from Sinopharm) and various extracts of natural products. Okras, aloe vera and avocado seeds are bought from local shops, green tea bags are bought from Rickshaw Chinese Teabag.

5.1.1.1 Okra

There were various methods of extraction for the okra, which made use of different structures of the plant.

5.1.1.1.1 Entire okra

To extract the okra using all of its structures, 200 g of the plant was boiled and put into a blender with 200 mL of distilled water. After blending, the mixture was filtered, such that only soluble substances were retained. The concentration of the solution was then measured.

Picture 1: putting the okra into the blender.

2022 S.-T. Yau High School Science Award
仅用于2022丘成桐中学科学奖公示

5.1.1.1.2 Mucilage

To extract the mucilage of the okra, the plant was put in boiling water briefly. Then, 200 mL of the mucilage was squeezed out of the central axis and then centrifuged to remove impurities. The concentration of the solution was then measured.

Picture 2: extracting the okra mucilage from its central axis

5.1.1.1.3 Central axis

To obtain an extract of the central axis of the okra, 200 g of the central axis was removed from the okra and put into a blender with 200 mL of distilled water. After blending, the mixture was filtered and centrifuged, such that the soluble substances were retained. The concentration of the solution was then measured.

Picture 3: removing the central axis from the okra

Picture 4: removing the seeds from the okra.

5.1.1.1.4 Seed

To obtain an extract of the seeds of the okra, 200 g of the seeds were removed from the okra and put into a blender with 200 mL of distilled water. After blending, the mixture was filtered and centrifuged, such that the soluble substances were retained. The concentration of the solution was then measured.

2022 S. Thomas' High School Science Award
仅用于中学生科学奖公开

5.1.2 Silver nanoparticles

For the synthesis of silver nanoparticles, a 5000 ppm $AgNO_3$ solution was prepared and used for all set-ups to produce 100 mL of 100 ppm AgNPs solution.

5.1.2.1 Starch

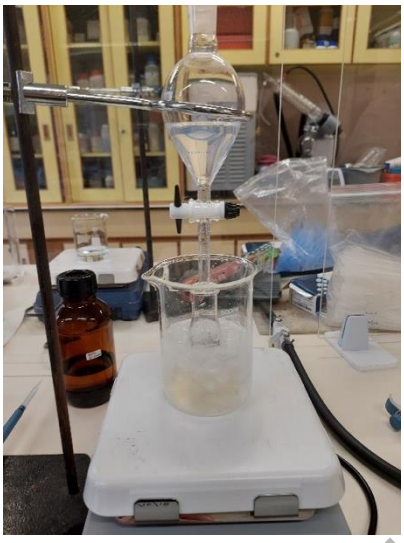

Picture 5: addition of starch-chelated silver ions into the sodium borohydride solution in an ice bath

To synthesize Starch/AgNPs, 0.5 g of starch was dissolved in 48 mL of boiling distilled water. 2 mL of the 5000 ppm $AgNO_3$ solution was added to the starch solution and stirred at room temperature. Then, 0.105 g of $NaBH_4$ was dissolved in 50 mL of distilled water in an ice bath. The mole ratio of Ag^+:$NaBH_4$ was 1:30, such that the reducing agent was in excess. Then, the starch-chelated silver ion solution was added dropwise to the $NaBH_4$ solution in the ice bath with stirring. The above procedures were repeated by adding the starch-chelated silver ion solution dropwise to 50 mL of 2% tea extract solution at room temperature with stirring.

5.1.2.2 Alginate

To synthesize Alginate/AgNPs, 0.5 g of sodium alginate was dissolved in 48 mL of distilled water. 2 mL of the 5000 ppm $AgNO_3$ solution was added to the alginate solution and stirred at room temperature. Then, 0.105 g of $NaBH_4$ was added to 50 mL of distilled water in an ice bath. The mole ratio of Ag^+:$NaBH_4$ was 1:30, such that the reducing agent was in excess. Then, the alginate-chelated silver ion solution was added dropwise to the $NaBH_4$ solution in the ice bath with stirring.

2022 S - T Yau High School Science Award
仅用于2022丘成桐中学科学奖公示

5.1.2.3 Chitosan

To synthesize Chitosan/AgNPs, 0.5 g of chitosan was added to 48 mL of distilled water. 0.3 mL of acetic acid was added to the mixture to dissolve the chitosan. 2 mL of the 5000 ppm $AgNO_3$ solution was added to the alginate solution and stirred at room temperature. Then, 0.105 g of $NaBH_4$ was added to 50 mL of distilled water in an ice bath. The mole ratio of Ag^+:$NaBH_4$ was 1:30, such that the reducing agent was in excess. Then, the chitosan-chelated silver ion solution was added dropwise to the $NaBH_4$ solution in the ice bath with stirring. The above procedures were repeated by adding the chitosan-chelated silver ion solution dropwise to 50 mL of 2% tea extract solution at room temperature with stirring.

5.1.2.4 Okra extract

To synthesize okra-reduced-and-chelated AgNPs, various amounts of the 4 types of okra extracts were prepared and diluted to a solution of 50 mL, such that they contained 0.5 g and 0.25 g of okra extracts respectively. For each concentration of each type of okra extract, 2 mL of the 5000 ppm $AgNO_3$ solution was made up to 50 mL, and added to the okra extract solution dropwise at room temperature with stirring.

To synthesize AgNPs using mixed okra extracts, 2 mL of the 5000 ppm $AgNO_3$ solution was made up to 50 mL, and added respectively to 3 sets of mixed okra extract solution dropwise at room temperature with stirring, such that the resultant solutions contained 0.25 g of okra central axis extract with 0.25 g of okra seed extract, 0.25 g of okra central axis extract with 0.125 g of okra seed extract and 0.125 g of okra central axis extract with 0.25 g of okra seed extract, respectively.

To synthesize okra-chelated AgNPs reduced by sodium borohydride, the 2 okra extracts that made use of the entire okra and its mucilage respectively were prepared and diluted to a solution of 48 mL, such that the mixtures contained 0.25 g of okra extracts each. 2 mL of the 5000 ppm $AgNO_3$ solution was added to the okra solution. Then, 0.011 g of $NaBH_4$ was added to 50 mL of distilled water in an ice bath. The mole ratio of Ag^+:$NaBH_4$ is 1:3, such that the reducing agent was in excess. Then, the okra-chelated silver ion solution was added dropwise to the $NaBH_4$ solution in the ice bath with stirring.

2022 S.T. Yau High School Science Award
仅用于2022丘成桐中学科学奖公示

5.1.2.5 No capping agent

As a control, silver nanoparticles were also synthesized without any capping agent. 2 mL of the 5000 ppm $AgNO_3$ solution was added to 48 mL of distilled water. Then, 0.105 g of $NaBH_4$ is added to 50 mL of distilled water in an ice bath. The mole ratio of Ag^+:$NaBH_4$ was 1:30, such that the reducing agent was in excess. Then, the silver ion solution was added dropwise to the $NaBH_4$ solution in the ice bath with stirring.

5.1.3 Copper nanoparticles

For the synthesis of copper nanoparticles, a 5000 ppm copper(II) chloride solution was prepared and used for all set-ups to produce 100 mL of 100 ppm CuNP solution. During and after the preparation of nanoparticle solutions, they were covered with aluminium foil to prevent oxidation of the CuNPs in the air to form copper(II) ions.

5.1.3.1 Starch

To synthesize starch-chelated CuNPs, 0.5 g of starch was dissolved in 48 mL of boiling distilled water. Then, 2 mL of 5000 ppm $CuCl_2$ solution was added into the starch solution at room temperature. Next, 0.832 g of L-ascorbic acid was added to 50 mL of distilled water. The mole ratio between copper(II) ions and L-ascorbic acid was 1:30, such that the reducing agent was in excess. Then, the solution of L-ascorbic acid was added dropwise to the starch-chelated copper(II) ion solution at 80°C with stirring.

5.1.3.2 Chitosan

To synthesize chitosan-chelated CuNPs, 0.5 g of chitosan was added to 48 mL of distilled water. 0.3 mL of acetic acid was added to the mixture to dissolve the chitosan. Then, 2 mL of 5000 ppm $CuCl_2$ solution was added into the chitosan solution. Next, 0.832 g of L-ascorbic acid is added to 50 mL of distilled water. The mole ratio between copper(II) ions and L-ascorbic acid was 1:30, such that the reducing agent was in excess. Then, the solution of L-ascorbic acid was added dropwise to the chitosan-chelated copper(II) ion solution at 80°C with stirring.

5.1.3.3 Okra extracts

To synthesize okra-reduced-and-chelated CuNPs, extracts of the okra mucilage and seeds were prepared and diluted to a solution of 50 mL, such that they contained 0.5 g and 0.25 g of okra extracts respectively. For each concentration of each type of

2022 S.-T. Yau High School Science Award
仅用于2022丘成桐中学科学奖公示

okra extract, 2 mL of the 5000 ppm $CuCl_2$ solution was made up to 50 mL, and added to the okra extract solution dropwise at room temperature with stirring.

To synthesize okra-chelated CuNPs reduced by sodium borohydride, the 2 okra extracts that made use of the okra seed and okra body respectively were prepared and diluted to a solution of 48 mL, such that the mixtures contained 0.05 g of okra extracts each. 2 mL of the 5000 ppm $CuCl_2$ solution was added to the okra solution. Then, 0.018 g of $NaBH_4$ was added to 50 mL of distilled water in an ice bath. The mole ratio of Ag^+:$NaBH_4$ is 1:3, such that the reducing agent was in excess. Then, the okra-chelated copper(II) ion solution was added dropwise to the $NaBH_4$ solution in the ice bath with stirring.

To synthesize okra-chelated CuNPs reduced by L-ascorbic acid, the 2 okra extracts that made use of the okra seed and okra central axis respectively were prepared and diluted to a solution of 48 mL, such that the mixtures contained 0.05 g of okra extracts each. 2 mL of the 5000 ppm $CuCl_2$ solution was added to the okra solution. Then, 0.139 g L-ascorbic acid was added to 50 mL of distilled water. The mole ratio of Ag^+:L-ascorbic acid was 1:5, such that the reducing agent was in excess. Then, the L-ascorbic solution was added dropwise to the okra-chelated copper(II) ion solution at 80°C with constant stirring.

5.1.3.4 L-ascorbic acid

To synthesize L-ascorbic acid-reduced-and-chelated CuNPs, 0.832 g of L-ascorbic acid was dissolved in 50 mL of distilled water. The mole ratio between copper(II) ions and L-ascorbic acid was 1:30, such that the reducing agent was in excess. Next, 2 mL of 5000 ppm $CuCl_2$ solution was added to 48 mL of distilled water and heated to 80°C. Then, the L-ascorbic acid solution was added dropwise to the copper(II) ion solution with stirring.

5.1.3.5 No capping agent

To synthesize copper nanoparticles without capping agents while using potassium iodide as a stabilizing agent, 0.022 g of $CuCl_2 \cdot 5H_2O$ was dissolved in 25 mL of water. 0.017 g or 0.002 g of KI was dissolved in 25 mL of distilled water respectively, such that the mole ratios of Cu^{2+}:KI to be added were 1:1 and 10:1 respectively. The KI solutions were then mixed with the Cu^{2+} solution. Then, 0.114 g of $NaBH_4$ was dissolved in 50 mL of ice-bathed water, such that the mole ratio of Cu^{2+}:$NaBH_4$ was

2022 S.T.Yau High School Science Award
仅用于2022丘成桐中学科学奖公示

1:6. The iodide and copper(II) ion solutions were added to ice-bathed $NaBH_4$ solutions respectively with constant stirring.

5.1.4 UV-Vis spectroscopy

For the successfully synthesized silver nanoparticles, a UV-Vis spectroscopy was conducted using an analyzer with the wavelength ranges from 300 nm to 900 nm, such that the successful formation of silver nanoparticles could be verified.

5.1.5 Nanoparticle tracking analysis

For the successfully synthesized silver nanoparticles, a nanoparticle tracking analysis (NTA) was conducted using a ZetaView nanoparticle tracking analyzer, such that the successful formation of silver nanoparticles could be verified, and their particle size and dispersity could be estimated.

5.2 Results

5.2.1 Silver nanoparticles

5.2.1.1 Starch

Using starch as a capping agent and sodium borohydride as a reducing agent, a clear brownish solution of Starch/AgNPs with no precipitates was obtained (Picture 6). It was generally stable, but precipitates were observed after about 1 month of storage at 4°C.

The UV-Vis absorbance spectroscopy showed that the curves of different concentrations all showed an absorption peak at 402 nm (Figure 2). The NTA carried out showed that the diameters of the Starch/AgNPs were mainly at 82.5 nm (Table 1).

On the other hand, using starch as a capping agent and tea extract as a reducing agent produced an unclear solution of greenish-brown colour with precipitates (Picture 7).

2022 S.-T. Yau High School Science Award
仅用于2022丘成桐中学科学奖公示

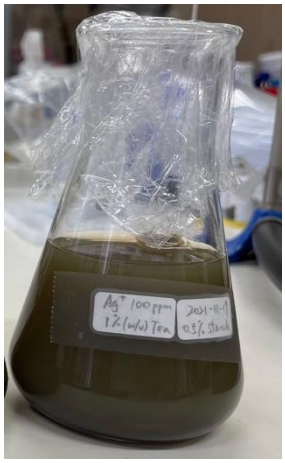

Picture 7: starch-capped and tea-extract-reduced Ag mixture

Picture 6: the borohydride reduced Starch/AgNPs

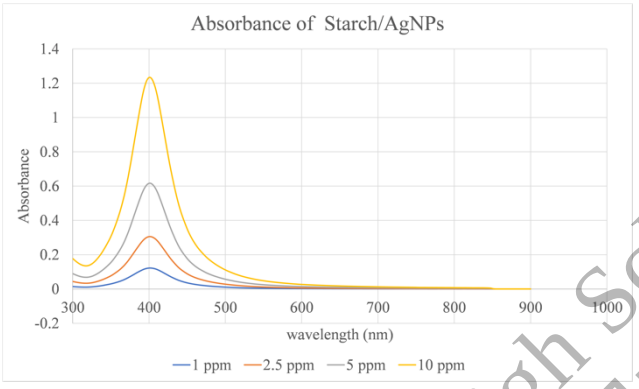

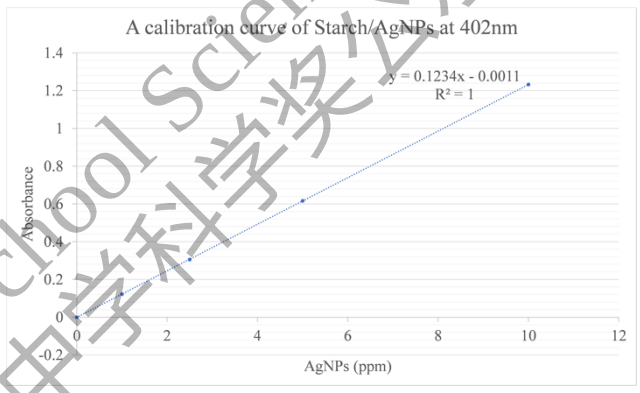

Figure 3: Left: the absorbance of Starch/AgNPs;
Right: the calibration curve of Starch/AgNPs at 402 nm

Figure 2:

Left: histogram showing the distribution of Starch/AgNPs by particle size;

Right: the NTA image of starch-chelated AgNPs

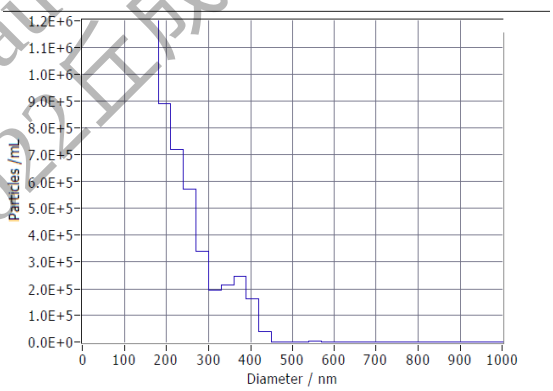

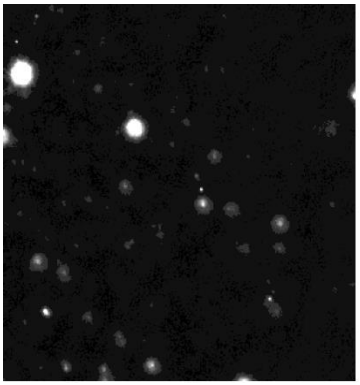

Peak analysis of NTA of Starch/AgNPs			
Diameter / nm	Particles / mL	FWHM / nm	Percentage / %
82.5	2.4E+6	152.3	100.0

Table 1: peak analysis of NTA of Starch/AgNPs

2022 S.T. Yau High School Science Award
仅用于2022丘成桐中学科学奖公示

5.2.1.2 Alginate

Using alginate as a capping agent and sodium borohydride as a reducing agent, a clear brownish solution of Alginate/AgNPs with no precipitates was obtained (Picture 8). It was generally stable, but a very small amount of precipitates were observed after about 1 month of storage at 4°C.

The UV-Vis absorbance spectroscopy showed that the curves of different concentrations all showed an absorption peak at 404 nm (Figure 4). The NTA carried out showed that the diameters of the Alginate/AgNPs were mainly at 84.8 nm (Table 2).

Picture 8: the sodium-borohydride reduced Alginate/AgNPs.

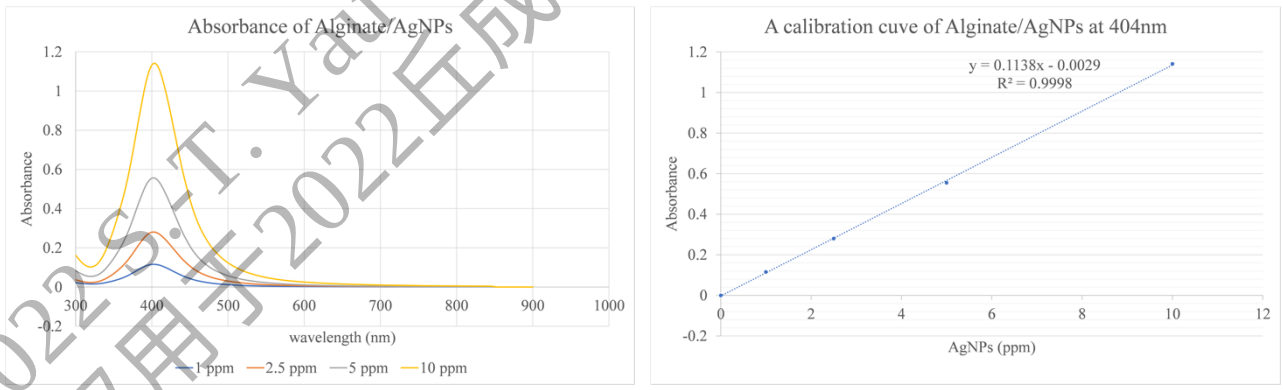

Figure 4: Left: the absorbance of Alginate/AgNPs.
Right: the calibration curve of Alginate/AgNPs at 404 nm.

2022 S.T. Yau High School Science Award
仅用于2022丘成桐中学科学奖公示

Figure 5:

Left: histogram showing the distribution of Alginate/AgNPs by particle size;
Right: the NTA image of Alginate/AgNPs.

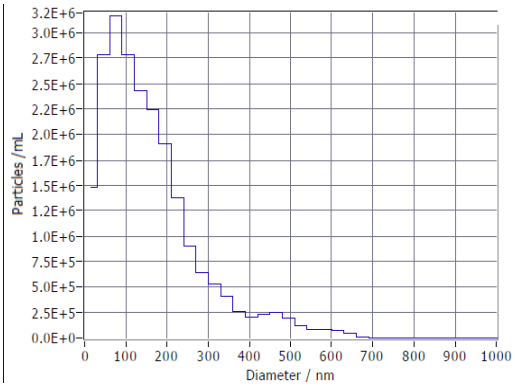

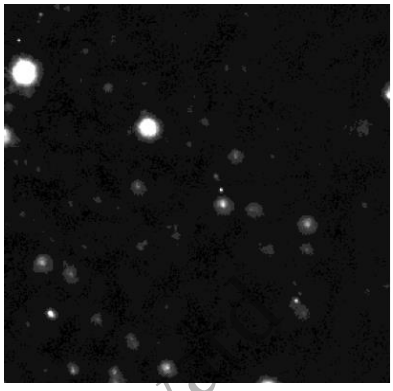

Peak analysis of NTA of Alginate/AgNPs			
Diameter / nm	Particles / mL	FWHM / nm	Percentage / %
84.8	3.0E+6	196.1	100.0

Table 2: peak analysis of NTA of Alginate/AgNPs

5.2.1.3 Chitosan

Using chitosan as a capping agent and sodium borohydride as a reducing agent, a clear dark brownish solution of Chitosan/AgNPs with no precipitates could be obtained (Picture 9). It was very stable, no precipitates were observed after about 1 month of storage at 4°C.

The UV-Vis absorbance spectroscopy showed that the curves of different concentrations showed an absorption peak at around 408 nm. On the other hand, using chitosan as a capping agent and tea extract as a reducing agent produced an unclear solution of dark greyish colour with precipitates (Picture 10).

Picture 9: the sodium-borohydride-reduced Chitosan/AgNPs.

Picture 10: chitosan-capped and tea-extract-reduced Ag mixture.

2022 S.T. Yau High School Science Award
仅用于2022丘成桐中学科学奖公示

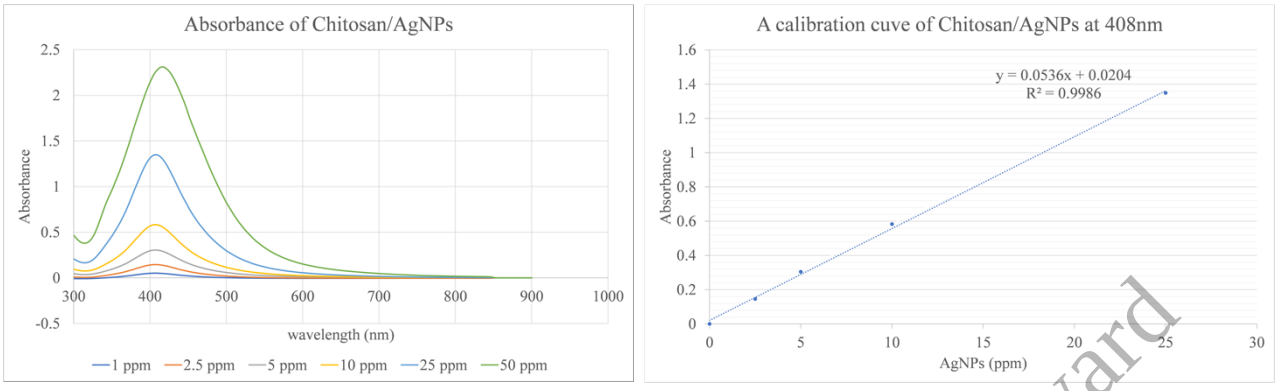

Figure 6: Left: the absorbance of Chitosan/AgNPs.
Right: the calibration curve of Chitosan/AgNPs at 408 nm.

5.2.1.4 Okra extract

Different concentrations of different types of okra extracts produced different results. When using okra mucilage as both the capping agent and the reducing agent, it was found that a 0.5% weight to volume ratio produced a clear reddish solution of silver nanoparticles with no precipitates (Picture 11), which was very stable, no precipitates were observed after about 3 months of storage at 4°C. A 0.25% concentration produced an unclear solution of orange colour with precipitates (Picture 12).

Picture 11: AgNPs capped and reduced by 0.5% okra mucilage.

Picture 12: AgNPs capped and reduced by 0.25% okra mucilage.

When using okra seeds as both the capping agent and the reducing agent, a 0.25% concentration produced a clear dark brownish solution of silver nanoparticles (Picture 13), while a 0.5% concentration produced an unclear solution with a similar colour (Picture 14).

The UV-Vis absorbance spectroscopy showed that the curves of different concentrations all showed an absorption peak at 416 nm (Figure 7). The NTA carried

2022 S.-T. Yau High School Science Award
仅用于2022丘成桐中学科学奖公示

out showed that the diameters of the okra seed-chelated silver nanoparticles (Okra/AgNPs) were mainly at 254.3 nm and 76.6 nm (Table 3).

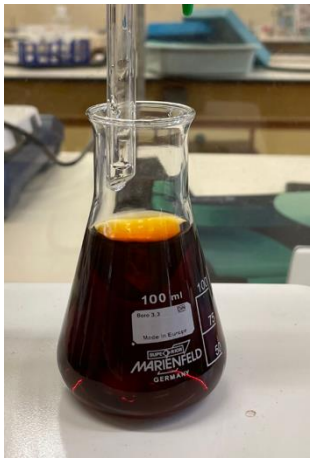

Picture 13: AgNPs capped and reduced by 0.25% okra seed

Picture 14: AgNPs capped and reduced by 0.5% okra seed.

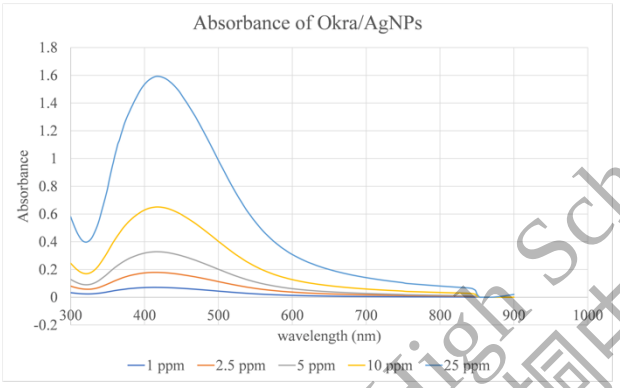

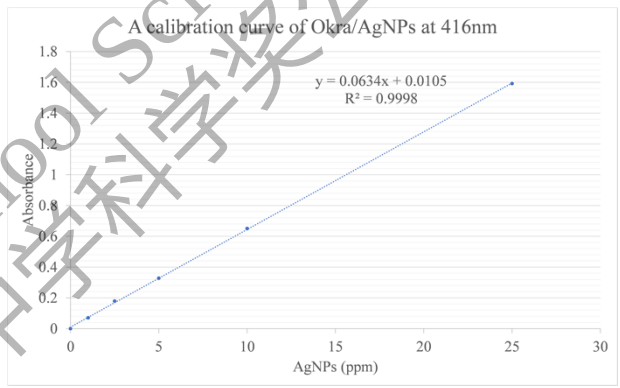

Figure 7: Left: the absorbance of Okra/AgNPs.
Right: the calibration curve of Okra/AgNPs at 416 nm.

Figure 8:

Left: histogram showing the distribution of Okra/AgNPs by particle size;

Right: the NTA image of Okra/AgNPs.

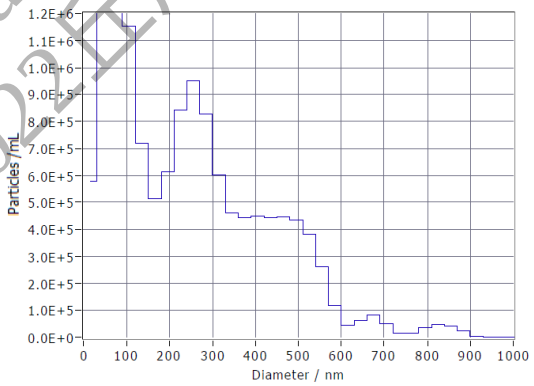

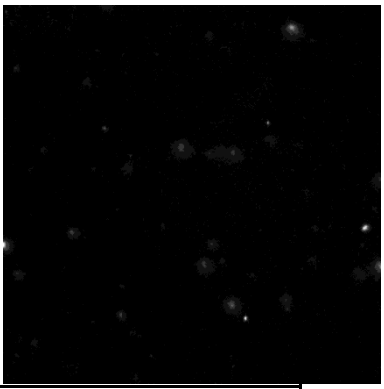

Peak analysis of NTA of Okra/AgNPs			
Diameter / nm	Particles / mL	FWHM / nm	Percentage / %
254.3	9.5E+5	147.1	58.0
76.6	1.4E+6	82.9	42.0

Table 3: peak analysis of NTA of Okra/AgNPs.

2023-T. Yau High School Science Award
仅用于2023丘成桐中学科学奖公示

All trials involving mixed okra extracts produced unclear yellowish solutions with precipitates (Picture 15).

Using okra mucilage as a capping agent and sodium borohydride as a reducing agent, a clear and very dark brownish solution of silver nanoparticles with no precipitates could be obtained. Using an extract of the entire okra as a capping agent and sodium borohydride as a reducing agent, a black solution with no precipitates could be obtained (Picture 16).

Picture 15: Left: Ag with 0.25% okra seed with 0.25% okra central axis (capping and reducing agent);
Middle: Ag with 0.25% okra seed with 0.125% okra central axis (capping and reducing agent);
Right: Ag with 0.125% okra seed with 0.25% okra central axis (capping and reducing agent).

Picture 16:

Left: Ag with 0.25% okra mucilage (capping agent) and sodium borohydride (reducing agent);

Right: Ag with 0.25% entire okra (capping agent) and sodium borohydride (reducing agent).

2022 S-T Yau High School Science Award
仅用于2022丘成桐中学科学奖

5.2.1.5 No capping agent

When the silver ion solution was reduced by a sodium borohydride solution without any capping agent, its colour turned from colourless to yellow, brown and eventually black, with precipitates (Picture 17).

Picture 17: Ag with sodium borohydride (reducing agent)

5.2.2 Copper nanoparticles

5.2.2.1 Starch

Using starch as a capping agent and L-ascorbic acid as a reducing agent, a clear pink solution was observed right after the addition of L-ascorbic acid had been completed. A pale orange colour was spotted after an hour and a half of constant heating and stirring while a golden yellow colour was observed after two hours of stirring (Picture 18). However, the stir bar was coated with reddish-brown copper precipitates.

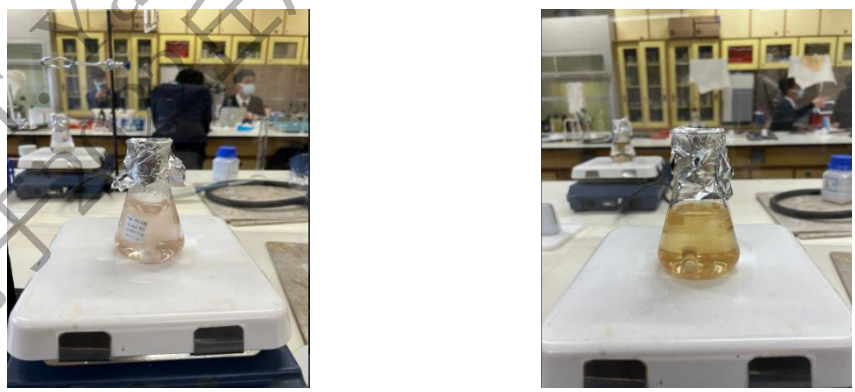

Picture 18: Cu with starch (capping agent) and L-ascorbic acid (reducing agent);
Left: right after the complete addition of all reactants;
Right: the solution after 1 hour of stirring and heating.

5.2.2.2 Chitosan

Using chitosan as a capping agent and L-ascorbic acid as a reducing agent, a clear pale reddish solution with brownish precipitates was obtained after the addition had

2022 S.T.Yau High School Science Award
仅用于2022年丘成桐中学科学奖公示

been completed (Picture 19). The colour of the solution turned to golden yellow after constant stirring and heating at 80°C.

Picture 19: Cu with chitosan (capping agent) and L-ascorbic acid (reducing agent).

5.2.2.3 Okra extracts

Using the mucilage as both the capping and reducing agent, a clear light blue solution was observed after the addition had been completed (Picture 20).

Picture 20: Cu with 0.25% okra mucilage (capping and reducing agent)

Using okra extracts as both the capping and reducing agent, the solution chelated with 0.25% mass to volume ratio of okra seed showed a light green colour right after addition, although an unclear brown solution was observed after a day of stirring and heating at 80°C. A 0.5% concentration produced a bluish-green solution right after completing the addition while an unclear dark brown solution was observed after a day of stirring and heating at 80°C (Picture 21).

2022 S.-T. Yau High School Science Award
仅用于2022丘成桐中学生科学奖公示

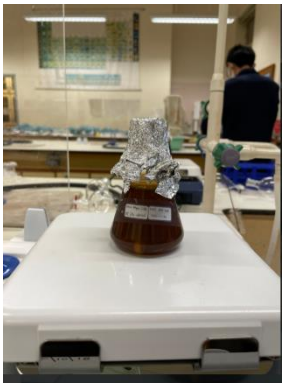
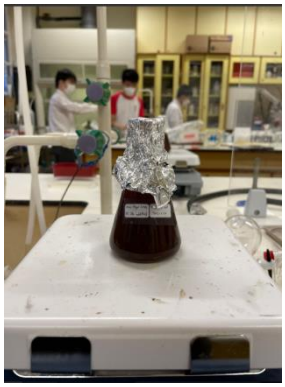

Picture 22: Left: Cu with 0.25% okra seed extract (capping and reducing agent);
Right: Cu with 0.5% okra seed extract (capping and reducing agent).

Using okra extracts only as the capping agent and sodium borohydride as the reducing agent, the solution of copper nanoparticles chelated by 0.05% okra seed extract showed a clear dark brown colour with no precipitates, while the one chelated by 0.05% okra central axis extract showed a clear light blue colour (Picture 22).

Picture 21: Left: Cu with okra seed (capping agent) and sodium borohydride (reducing agent);
Right: Cu with okra central axis (capping agent) and sodium borohydride (reducing agent)

Using okra extracts only as the capping agent and L-ascorbic acid as the reducing agent, the solution of copper nanoparticles chelated by 0.5% okra seed extract showed an unclear dark reddish-brown colour, while the one chelated by 0.5% okra central axis extract showed an unclear light yellow colour, both with reddish-brown precipitates observed (Picture 23).

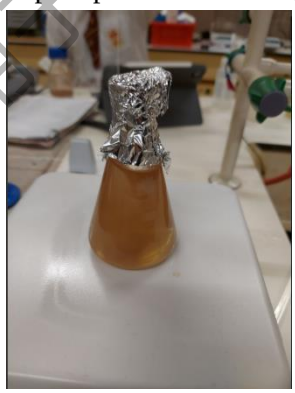


Picture 23: Left: Cu with okra seed (capping agent) and L-ascorbic (reducing agent);
Right: Cu with okra central axis (capping agent) and L-ascorbic (reducing agent).

2022 S.T.Yau High School Science Award
仅用于2022丘成桐中学生数学奖

5.2.2.4 L-ascorbic acid

Using L-ascorbic acid as both the capping and reducing agent, a clear golden yellow solution with reddish-brown precipitates was observed (Picture 24).

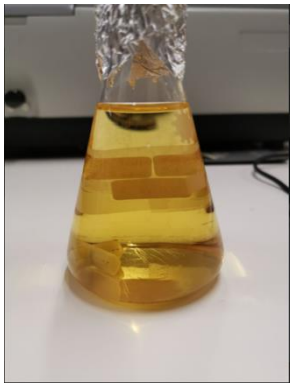

Picture 24: Cu with L-ascorbic acid (capping and reducing agent)

5.2.2.5 No capping agent

Using potassium iodide as the stabilizing agent and sodium borohydride as the reducing agent, both set-ups show a clear colourless solution with a lot of precipitates. Orange precipitates were observed in the solution with the mole ratio of Cu^{2+}:KI of 1:1. Green precipitates were observed in the solution with the mole ratio of Cu^{2+}:KI of 10:1 (Picture 25).

Picture 25:

Left: Cu with potassium iodide (stabilizing agent) (Cu^{2+}:KI of 1:1) and sodium borohydride (reducing agent);

Right: Cu with potassium iodide (stabilizing agent) (Cu^{2+}:KI of 10:1) and sodium borohydride (reducing agent).

2022 S.T. Yau High School Science Award
仅用于2022丘成桐中学科学奖公示

5.3 Discussion

5.3.1 Silver nanoparticles

5.3.1.1 Starch/Alginate/Chitosan/Sodium Borohydride

For the synthesis of silver nanoparticles, it is concluded that starch, alginate and chitosan are reliable capping agents. The carboxylate ions and polar functional groups of these compounds, namely the hydroxyl groups and the amine groups, can form dative covalent bonds with the silver ions, and interact with the hydroxyl groups and silver and oxide ions on the surface of the reduced silver nanoparticles, preventing them from collision and hence congregation [19]. The following diagrams show the proposed capping mechanisms for starch [20], alginate [21], chitosan [22].

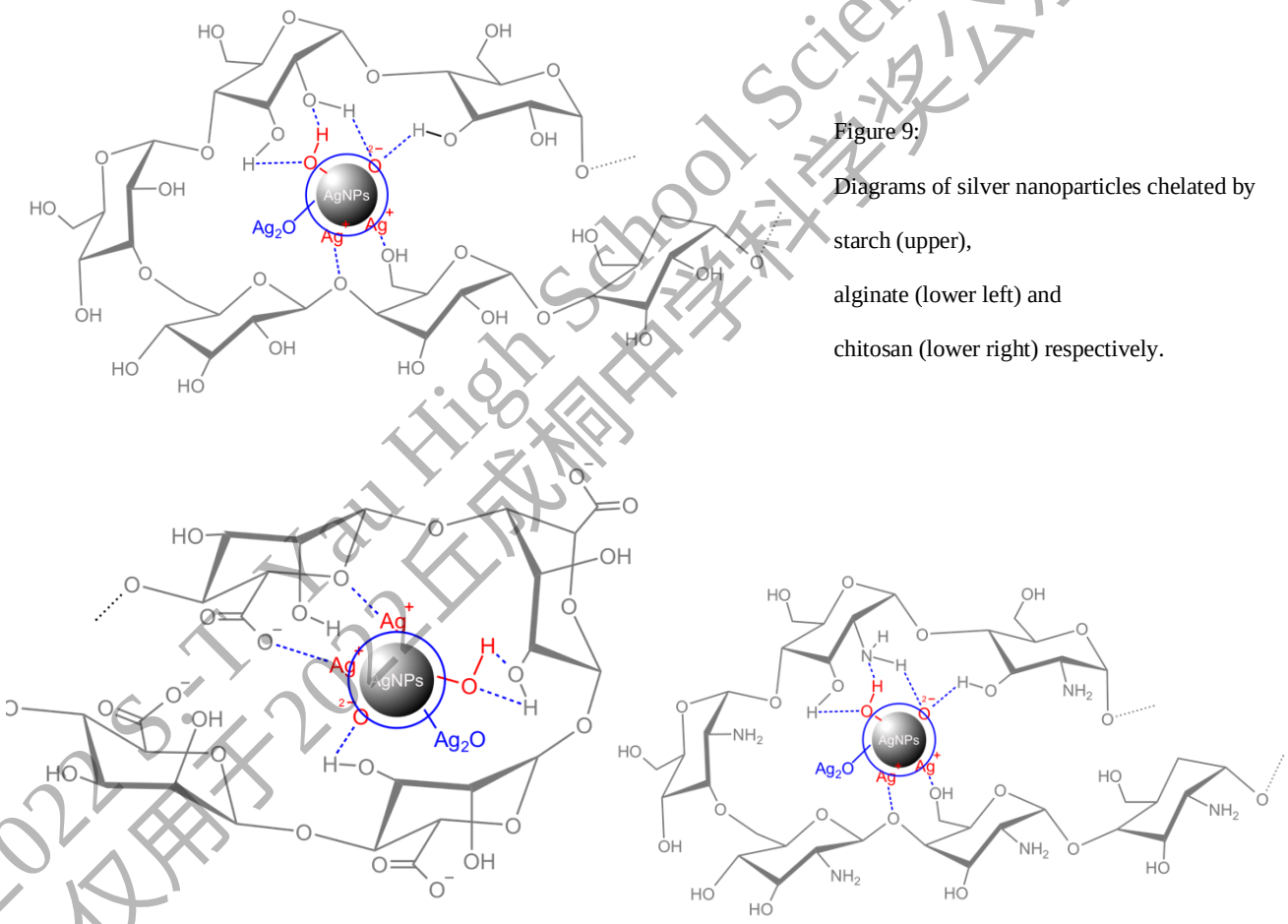

Figure 9:

Diagrams of silver nanoparticles chelated by

starch (upper),

alginate (lower left) and

chitosan (lower right) respectively.

These capping agents are best paired with sodium borohydride, a reliable reducing agent. However, it is noted that the sodium borohydride used must be largely in excess and be in an ice bath, or it will react with atmospheric air and be oxidized quickly, without reducing the silver ions.

Equation 2

$$2\,Ag^{+} + 2\,BH_4^{-} \longrightarrow 2\,Ag + 2\,BH_3 + H_2$$

2022 S.T.Yau High School Science Award
仅用于2022丘成桐中学科学奖公示

The UV-Vis absorbance spectroscopy conducted all showed absorption peaks at around 400 nm, indicating the successful formation of silver nanoparticles. However, it was noted that Starch/AgNPs had the most uniform dispersity according to the result of NTA, followed by Alginate/AgNPs, while those chelated by 0.5% okra seed extract have the most non-uniform dispersity.

5.3.1.2 Okra extracts

It is suggested that the oligosaccharides present in the okra mucilage, such as the homogalacturonan and the rhamnogalacturonan, can exhibit both capping and reducing capabilities. Their polar functional groups, such as the hydroxyl and ether groups, can form dative covalent bonds with the silver ions, and interact with the hydroxyl groups and silver and oxide ions on the surface of the reduced silver nanoparticles, preventing them from collision and hence congregation. On the other hand, their aldehyde ends can act as a reducing agent. As the sizes of these oligosaccharides lie between that of disaccharides and polysaccharides, they simultaneously possess sufficient capping lone pairs and reducing aldehyde ends, allowing one-pot synthesis. The following diagram shows the proposed capping mechanisms.

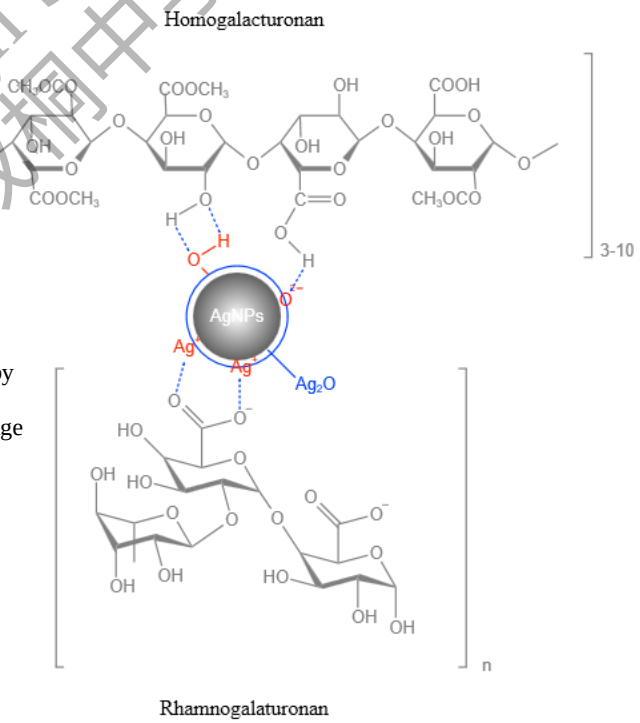

Figure 10:

Diagrams of silver nanoparticles chelated by oligosaccharides present in the okra mucilage

Sodium borohydride is apparently a suitable reducing agent for okra-chelated silver ions as well. It is noted that when okra extracts are used as the reducing agent, the reduction of the silver ions takes a longer time when compared to other set-ups involving sodium borohydride.

2022 S.T. Yau High School Science Award
仅用于2022丘成桐中学科学奖公示

Peak analysis of NTA of Starch, Alginate and Okra/AgNPs				
	Diameter / nm	Particles / mL	FWHM / nm	Percentage / %
Starch/AgNPs	82.5	2.4E+6	152.3	100.0
Alginate/AgNPs	84.8	3.0E+6	196.1	100.0
Okra/AgNPs (Peak 1)	254.3	9.5E+5	147.1	58.0
Okra/AgNPs (Peak 2)	76.6	1.4E+6	82.9	42.0

Table 4

A NTA was conducted on the Starch/, Alginate/ and Okra/AgNPs. It was noted that the full width at half maximum of the peak of Starch/AgNPs was smaller than that of the Alginate/AgNPs, while the Okra/AgNPs even showed two peaks of different particle sizes, so it was concluded that the ones synthesized with starch had the most uniform dispersity, followed by the ones with alginate, and then okra.

5.3.1.3 No capping agents

The control set-up with no capping agent resulted in a black colour, indicating that a capping agent is indeed necessary.

5.3.2 Copper nanoparticles

With respect to the experiments done, unlike silver nanoparticles, copper nanoparticles are unstable. It is concluded that copper nanoparticles will oxidize quickly once they are in contact with air to form copper(I) oxide. The copper(I) ions then oxidize to produce CuO^{2+} ions, which decompose into copper(II) ions and super oxide ions, as shown in the equation below [23].

Equation 3

$$4\,Cu + O_2 \longrightarrow 2\,Cu_2O$$
$$Cu^+ + O_2 \longrightarrow CuO_2{}^+$$
$$CuO_2{}^+ \longrightarrow Cu^{2+} + O_2{}^-$$

An aluminium foil must be used to cover the mouth of the conical flasks containing the CuNPs during the experiments. Although they can be synthesized, if they re-oxidize while being applied onto the hydrogels, they will not possess any antibacterial properties. Therefore, its sterilizing properties are not to be examined in the bacterial experiments.

2022 S.T.Yau High School Science Award
仅用于2022丘成桐中学科学奖公示

5.3.2.1 Starch/Chitosan/L-ascorbic acid

Two main reducing agents, namely sodium borohydride and L-ascorbic acid, had been selected to reduce copper(II) ions into CuNPs. Yet, for the set-ups using sodium borohydride, most of them failed as the reducing power of sodium borohydride was too strong, creating a lot of reddish-brown copper precipitates. Therefore, L-ascorbic acid, which possesses sufficient reducing power when the temperature reaches 80°C, is preferred for the synthesis of copper nanoparticles.

In general, it took about 16 h of constant heating and stirring for copper nanoparticles to form. Furthermore, no matter what capping agents and reducing agents were adopted, reddish brown precipitates were often observed, either on the stir bar or on the periphery of the conical flask. This indicated the loss of a certain amount of copper metal. Nevertheless, clear solutions in a golden yellow colour are observed when starch, chitosan and L-ascorbic acid were used as the capping agents with L-ascorbic acids as the reducing agent, indicating the presence of copper nanoparticles.

5.3.2.2 Okra extracts

For the okra extracts, only the okra seed extract was proved to be capable of capping the copper nanoparticles as shown in the set-ups using an okra seed extract as the capping agent and sodium borohydride as the reducing agent. On the other hand, when the other okra extracts involving its mucilage, seed and central axis, were used as the reducing agent and capping agent simultaneously, the appearance of the solutions did not indicate the successful formation of copper nanoparticles. The one with the okra mucilage turned out with a blue colour, showing that the copper(II) ions were not reduced, while the ones with okra seed and central axis extracts developed an unclear brown colour. In short, the okra seed extract is a suitable capping agent for the formation of copper nanoparticles when a strong reducing agent such as sodium borohydride is used, but it itself is not a good reducing agent for copper nanoparticles. For the mucilage and central axis extracts, no evidence has been found to show that they are good capping agents for the synthesis of copper nanoparticles.

5.3.2.3 No capping agents

The control set-up with no capping agent resulted in a lot of precipitates, indicating that a capping agent is indeed necessary. Iodide ions react with copper(II) ions to form a layer to CuI to stabilize. Yet, side reactions occur and CuNPs are not successfully capped.

2022 S.T. Yau High School Science Award
仅用于2022丘成桐中学科学奖公示

6 Antibacterial activity test

6.1 Experimental

6.1.1 Materials

To make 1 L lysogeny broth, or Luria-Bertani medium (LB), 10 g tryptone (purchased from aladdin), 5 g yeast extract and10 g NaCl (purchased from UNI-CHEM) were added to 1L of distilled water and boiled. To make LB agar, the 1 L LB solution were added with 15 g of agar powder (purchased from UNI-CHEM) and boiled to obtain a clear solution. The solution was poured into the Petri dish and the agar formed after cooling. All apparatus was sterile and the experiment was conducted in a sterile environment.

6.1.2 Modified disc-diffusion assay

A modified disc-diffusion method was carried out to determine the antibacterial activity of the synthesized NPs. Gram-negative bacteria E. coli was used as the bacterial model in the test. 50 μL of E. coli cultured LB, was added to each of the Petri dishes containing LB agar and spread evenly. 10 μL of each of the test samples was added vertically and directly onto the agar, and the Petri dishes were incubated at 36°C for 24 h. The zones of inhibition were observed and their diameters were measured.

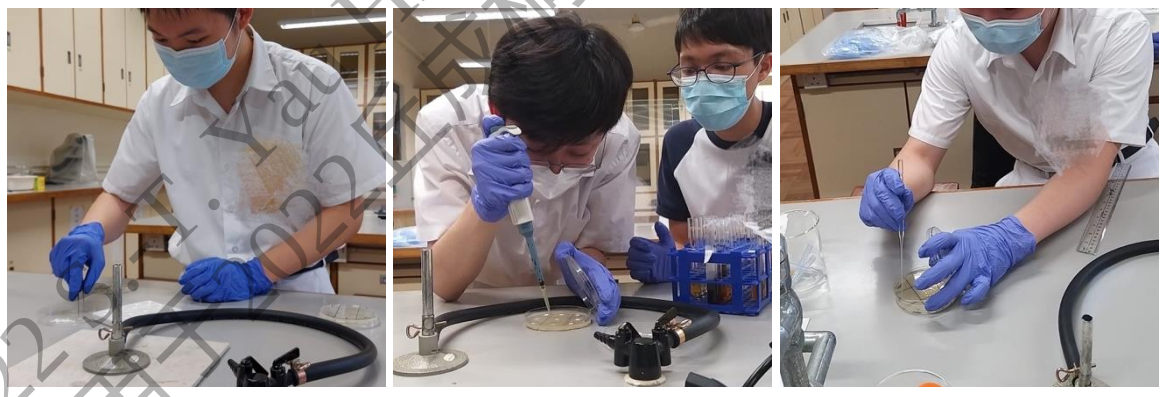

Picture 28: conducting modified disc-diffusion assay

Picture 27: Chitosan/AgNPs precipitated out in LB.

Picture 26: Left: adding E. coli into cuvette;
Middle: measuring the OD600;
Right: cuvettes added with micromagnetic stir bars.

2022 第十一届 Yau High School Science Award 仅用于2022年中国中学科学奖公示

6.1.3 OD_{600} quantitative analysis

To quantitively evaluate the antibacterial effect of the synthesized NPs, and monitor their antibacterial process, OD_{600} quantitative analysis was carried out.

To determine the inhibition ratio and minimum inhibitory concentration MIC, optical densities at λ = 600 nm (OD_{600}) of E. coli added with various test samples, were measured in cuvettes at regular time intervals. 600-nm wavelength was chosen as it is not harmful to E. coli, and is usually not absorbed by LB. The cultured E. coli was diluted with LB to obtain an OD_{600} of about 0.2. Each cuvette was added with 2.5 mL of the E. coli solution, followed by 0.5 mL of the test samples, respectively, as listed below:

	Type	Conc.	Unit
NP solution	Starch/AgNPs and Alginate/AgNPs	100	ppm
		50	
		25	
		10	
		5	
		2.5	
		1	
Background of NP solution	Starch slon (0.5%) and Alginate soln (0.5%)	100	% (v/v)
		50	
		10	
		1	
	Alcohol (isopropanol)	0.75	%
	Distilled water		
Control	LB		

A micromagnetic stir bar was added to each cuvette and the solution was stirred on a magnetic stir plate at 1500 rpm. All cuvettes were incubated at 36°C, and the OD_{600} were measured every hour （Picture 28）. The first recorded values were treated as zero for correction purposes (as the addition of the test samples would affect the OD_{600}), and the accumulative changes of OD_{600} of each set were measured. The inhibition ratio was calculated as shown in the following equation:

Equation 4

$$Inhibition\ Ratio = \frac{OD_{control} - OD_{test\ sample}}{OD_{control}} \times 100\%$$

The MIC was determined by finding the set with the lowest concentration of AgNPs that experienced no OD_{600} increment in the test.

2022 S.T. Yau High School Science Award
仅用于2022丘成桐中学科学奖公示

In this test, Okra/AgNPs were not included because of their low antibacterial effect in the disc-diffusion assay. Chitosan/AgNPs were also not included, but it was due to the low solubility of chitosan in neutral pH (with LB having a pH around 7). Furthermore, Chitosan/AgNPs precipitated out when added into LB, forming red insoluble clusters in the cuvette (Picture 26).

6.2 Result

6.2.1 Modified disc-diffusion assay

The diameters of inhibition zones are listed in Table 4. Notably, 0.5% of chitosan solution with acetic acid had an inhibition zone of 5 mm but this was significantly smaller than the one with 100 ppm of Chitosan/AgNPs (11 mm). The Petri dishes were further incubated at 36°C for another 8 days and no changes in the diameters of the inhibition zones were observed (Picture 29).

Test Samples	Conc.	Diameter (mm)
Starch/AgNPs	100 ppm	13
	50 ppm	10
	25 ppm	8
Alginate/AgNPs	100 ppm	10
	50 ppm	10
	25 ppm	8
Chitosan/AgNPs	100 ppm	11
	50 ppm	10
	25 ppm	10
	10 ppm	9
Okra-0.5%/AgNPs	100 ppm	0
Okra-0.25%/AgNPs	100 ppm	12
Starch Soln	0.50%	0
Alginate Soln	0.50%	0
Chitosan Soln with acetic acid	0.50%	5
Okra extract	0.50%	0
Isopropanol	75%	11
distilled water		0

Table 5: the results of the disc-diffusion essay. Except for the highest concentration, test samples with zero inhibition zones are not shown.

2022 S.T. Yau High School Science Award
仅用于2022丘成桐中学科学奖公示

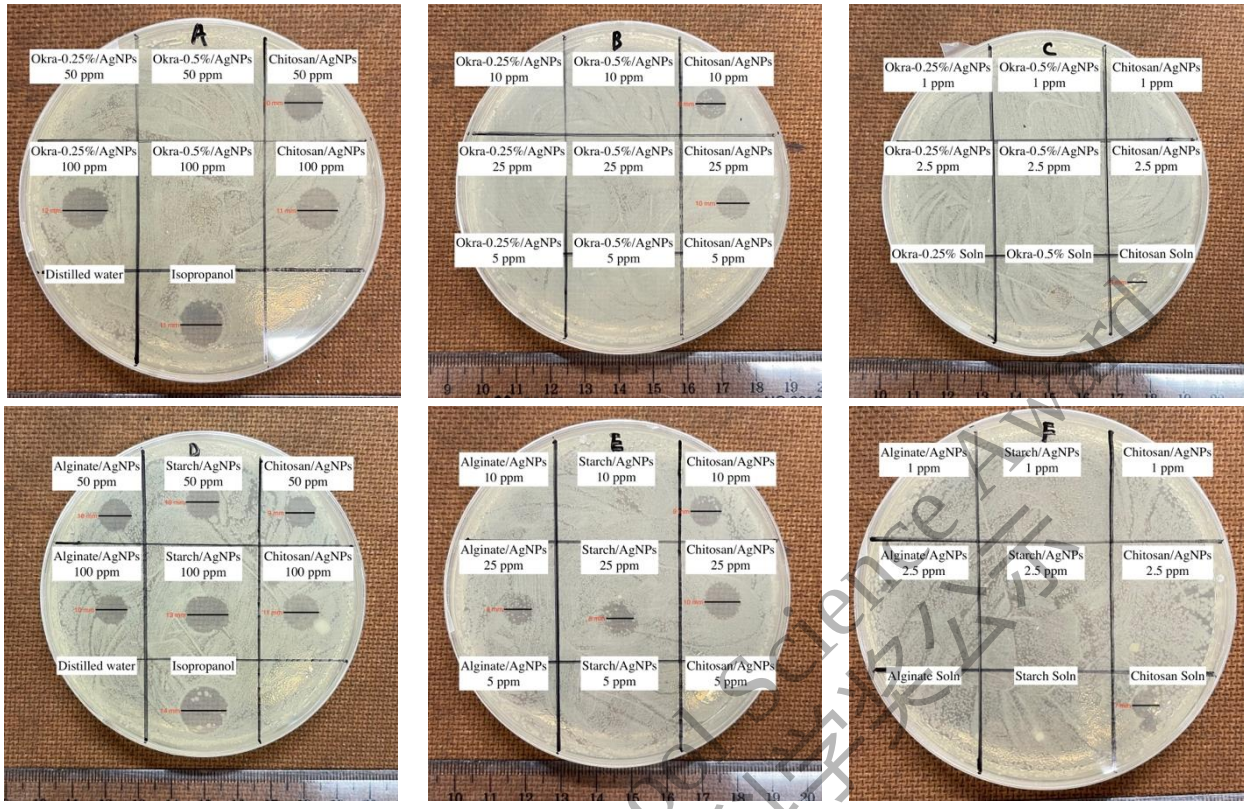

Picture 29: the Petri dishes of the disc-diffusion essay

6.2.2 OD600 quantitative analysis

In aqueous media, Starch/AgNPs showed a 100% inhibition ratio in the concentrations of 4.17, 8.33 and 16.7 ppm, with slightly negative OD600 changes (Figure 11). Starch/AgNPs of 1.67 ppm, which had a mean inhibition ratio of 58.8%, divided the graph into two halves: the samples below it were those that totally inhibited the growth of E. coli; the samples above it were those that exhibited little or no inhibitory effect. A negative inhibition ratio was recorded in the E. coli co-cultured with 0.083% starch solution, showing a faster bacteria growth in the starch solution than in LB (Figure 15).

The MIC of Starch/AgNPs was 4.17 ppm. However, the 100% inhibition ratio was reached after the fourth hour of incubation (Figure 19). In contrast, the NPs of 8.33, 16.7 ppm reached a 100% inhibition ratio in the first hour of measurement (data not shown). Notably, the inhibition ratios of the NPs below the MIC (0.17, 0.42, 0.83 and 1.67 ppm) showed a decreasing trend over time in general, especially in 1.67 and 0.83 ppm (Figure 17).

2022 S.-T. Yau High School Science Award
仅用于2022丘成桐中学科学奖

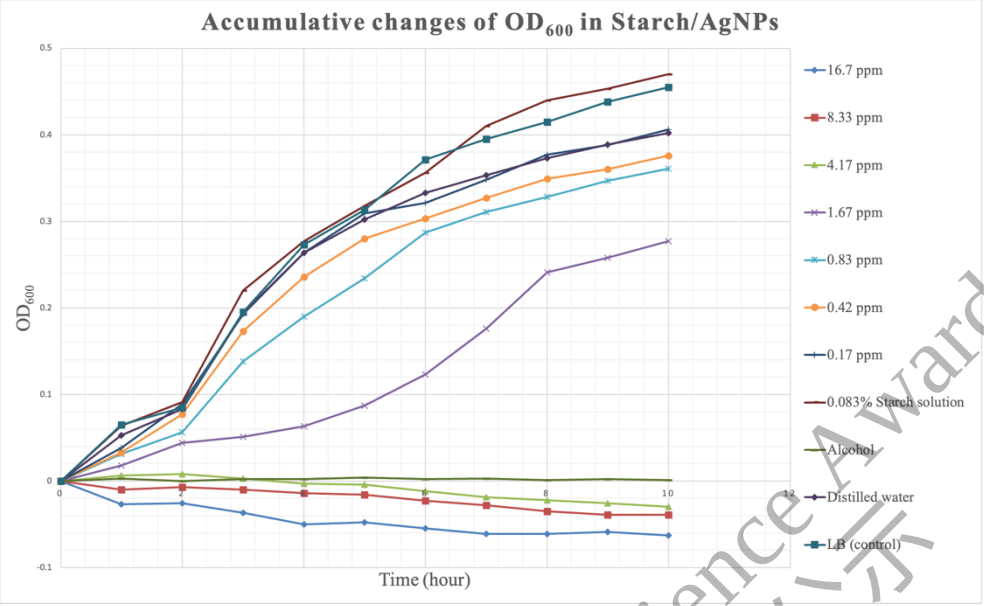

Figure 11

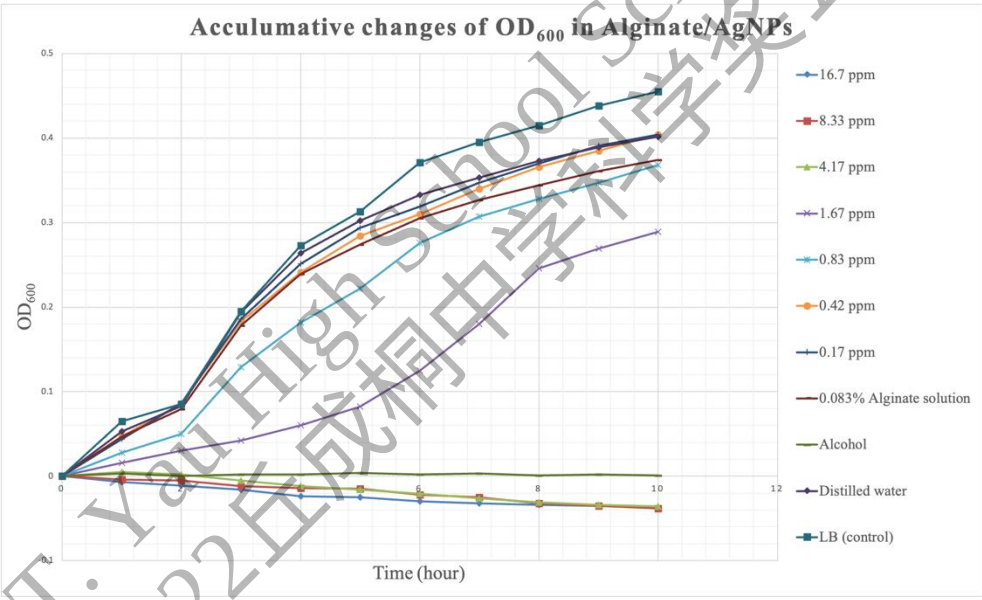

Figure 12

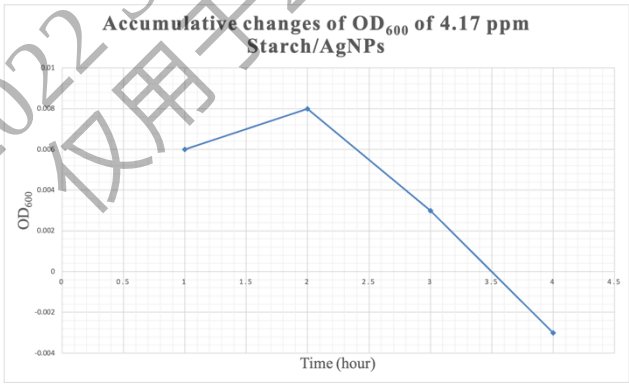

Figure 13

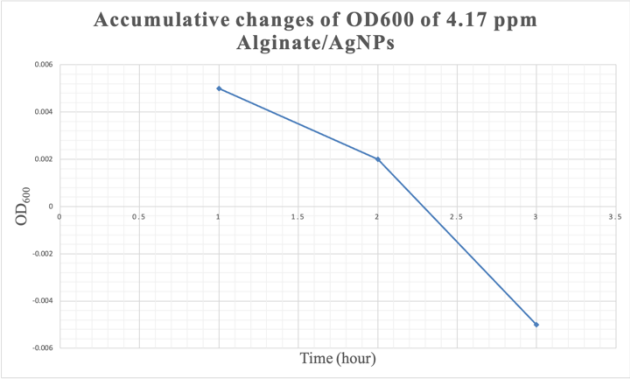

Figure 14

2022 S.T. Yau High School Science Award
仅用于2022丘成桐中学科学奖公示

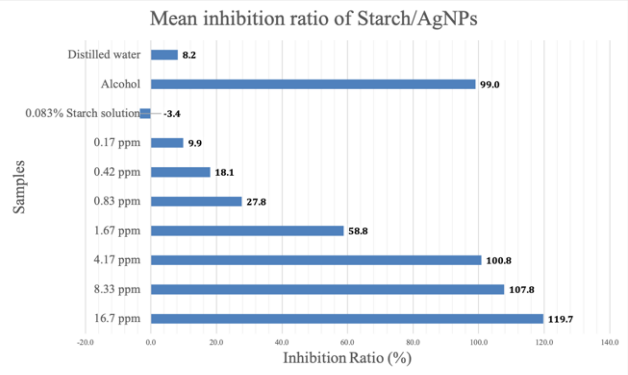

Figure 15

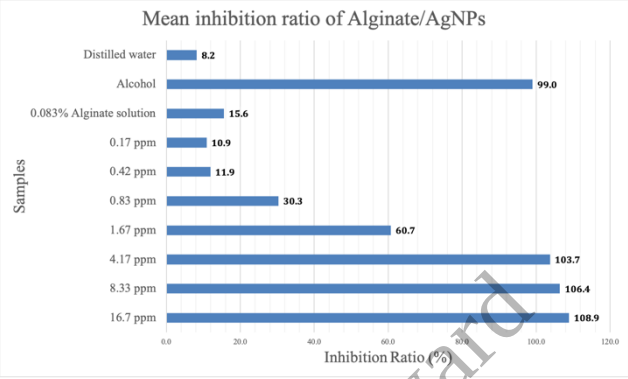

Figure 16

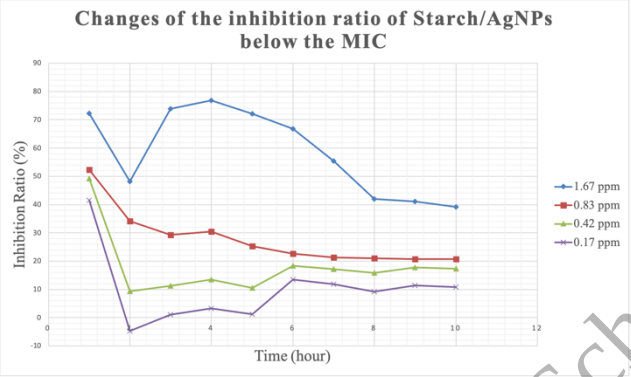

Figure 17

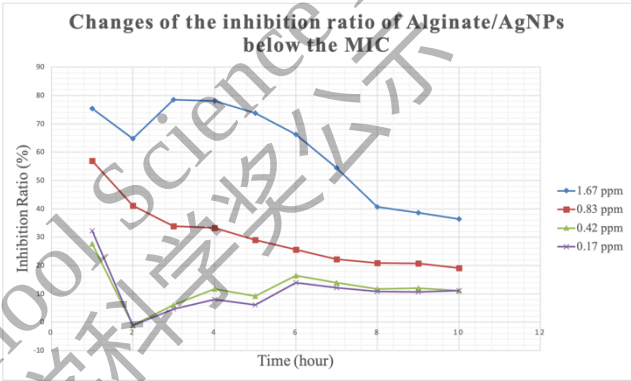

Figure 18

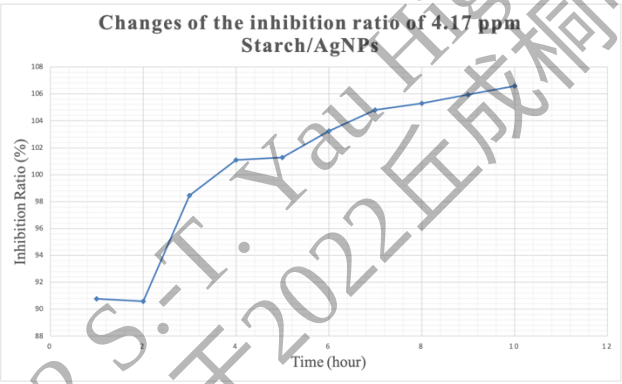

Figure 19

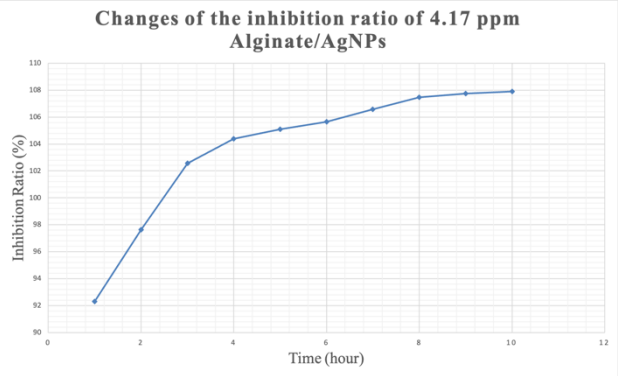

Figure 20

2022 S.-T. Yau High School Science Award
仅用于2022丘成桐中学科学奖公示

A very similar result (Figure 12) was obtained in Alginate/AgNPs, except a relatively strong inhibition ratio (15.6%) was obtained in the E. coli co-cultured with 0.083% alginate solution (Figure 16), which was higher than that of 0.17 and 0.42 ppm of Alginate/AgNPs.

Besides, in the MIC (4.17 ppm) of Alginate/AgNPs, the 100% inhibition ratio was reached after the third hour, earlier than that of the MIC of Starch/AgNPs, and the inhibition ratio rose continuously throughout the first 3 hours (Figure 20). Similarly,

concentrations below the MIC (0.17, 0.42, 0.83 and 1.67 ppm) also showed a decreasing trend over time (Figure 18).

6.3 Discussion

6.3.1 Modified disc-diffusion assay

With respect to the minimum concentration that could inhibit bacteria growth, it was found that Chitosan/AgNPs had the strongest inhibitory effect against E. coli, followed by Starch/AgNPs and Alginate/AgNPs. Okra-0.25%/AgNPs had very little effect on E. coli, but Okra-0.5%/AgNPs exhibited no inhibitory effect against E. coli at the concentration of 100 ppm.

It is believed that the size has a strong influence on the antibacterial activity of AgNPs. On one hand, the smaller the particles, the easier they can physically penetrate E. coli. On the other hand, the smaller the size, the larger the surface area to volume ratio, and hence the faster the release of Ag^+ ions.

From the results of the particle tracking analyzer, the diameter of Starch/AgNPs and Alginate/AgNPs were mostly around 80 nm. However, Okra/AgNPs were mainly of 2 diameters, 254.3 and 76.6 nm, and they are roughly of equal number. Hence, AgNPs with a diameter of 254.3 nm are of a larger volume, which have a low antibacterial effect. Therefore, Okra/AgNPs had a much lower antibacterial effect than the other NPs in this test. Nevertheless, the Okra extract can be further purified to obtain a suitable capping agent which may have a better stabilizing effect to enhance the antibacterial activity in future research.

When compared by the structure of their cell walls, gram-negative bacteria are more susceptible to the attack of AgNPs, as gram-positive bacteria have thicker peptidoglycan composed of short peptides cross-linked by linear polysaccharides [24].

2022 S.T. Yau High School Science Award
仅用于2022正成国际科学奖公示

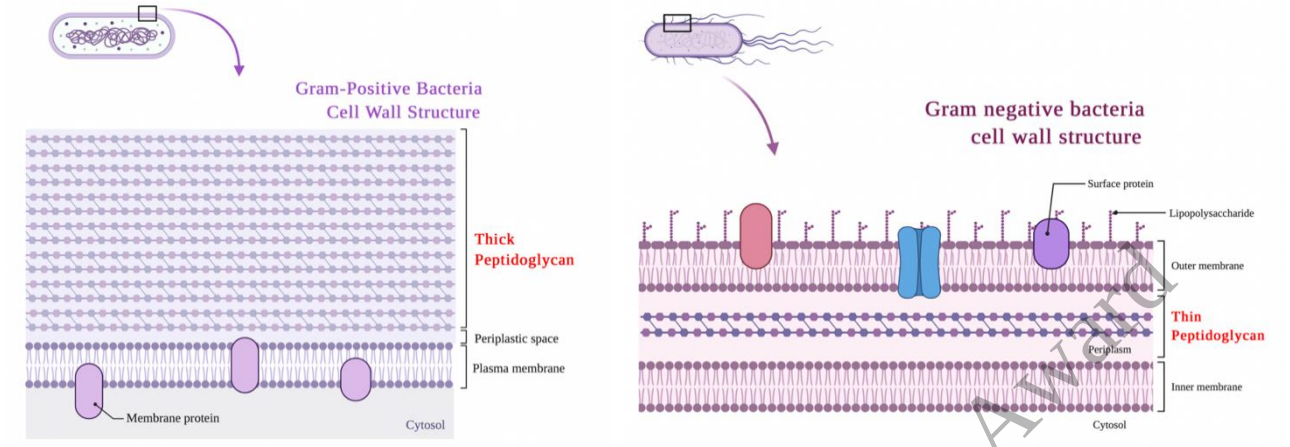

Figure 21: the simplified cell wall structure of (Left) gram-positive bacteria and (Right) gram-negative bacteria. Generated from BioRender.

The formation of the inhibition zone in the one added with chitosan/acetic acid solution is due to its known antiseptic effect. This might be caused by acid stress assaulting the E. coli, in which the acetic acid molecules diffuse into the cell membrane of E. coli, ionizing intracellularly and lowering the intracellular pH [25]. This would then denature the proteins inside and disturb the intracellular metabolism.

However, it is proposed that the acid stress did not play an important role in the antibacterial effect of Chitosan/AgNPs. As the Chitosan/acetic acid/Ag^+ mixture was added to the $NaBH_4$ solution, the acetic acid continued to ionize to produce H^+ ions, which then readily neutralized with the OH^- ions formed by the reaction between $NaBH_4$ and H_2O.

Equation 5

$$CH_3COOH \rightleftharpoons H^+ + CH_3COO^-$$
$$BH_4^- + H_2O \longrightarrow BH_3 + OH^- + H_2$$
$$H^+ + OH^- \longrightarrow H_2O$$

As a result, most of the acetic acid was consumed in the process, hence the concentration of acetic acid molecules present in the Chitosan/AgNPs was very low. The inhibitory effect of Chitosan/AgNPs could be solely explained by the antibacterial property of AgNPs.

To explain why Chitosan/AgNPs had a higher inhibitory effect, it is proposed that the pH of Chitosan/AgNPs (pH ≈ 4.5) is significantly lower than that of the others (pH ≈ 7), hence promoting the release of Ag^+ ions [11].

2022 S.-T. Yau High School Science Award
仅用于2022丘成桐中学科学奖公示

6.3.2 OD_{600} quantitative analysis

The results of both of the NPs were very similar, indicating that they had a similar antibacterial property and effect, which was also reflected in the disc-diffusion assay.

In the concentrations of 4.17, 8.33 and 16.7 ppm, the accumulative changes in OD_{600} were negative (Figures 11 and 12), leading to inhibition ratios over 100% (Figures 15 and 16). Hence, a control experiment using 100 ppm Starch/AgNPs as a test sample, without adding E. coli (LB only), was carried out to determine whether or not the E. coli was the factor leading to the negative OD_{600}. However, a non-negative OD_{600} change was observed after 1 hour of incubation (data not shown). Therefore, it was hypothesized that the negative value was due to the adhesion between AgNPs/Ag^+ ions and the E. coli organelles, via various mechanisms mentioned in the previous section.

From the results, the antibacterial activity can be divided into the stage of inhibition and sterilization [26]. In the inhibition stage, AgNPs firstly perforate the cell wall and membrane, resulting in bacteriolysis and the disturbance of cell replication. The rate of death of E. coli is roughly equal to the rate of reproduction, which is very likely the reason for the non-increasing inhibition ratio of Starch/AgNPs at MIC in the first 2 hours (Figure 19). However, the inhibition ratio of Alginate/AgNPs continued to increase (Figure 20), showing a stronger antibacterial effect. In the stage of sterilization, AgNPs kill the rest of the E. coli.

In the E. coli co-cultured with distilled water, LB, alcohol and AgNPs with concentrations between 0.17 and 0.83 ppm, a significant log phase (exponential growth) was observed between the first and the third hour (Figures 11 and 12). In the concentration of 1.67 ppm, it could be clearly seen that the E. coli was in the log phase from the second to the eighth hour. The log phase of E. coli was delayed and prolonged in this concentration. From Figures 17 and 18, the general decreasing inhibition ratio may reflect that the antibacterial activities of NPs are not catalytic. Hence, further research could be carried out to enhance the antibacterial effect by using dye-sensitized NPs which can continue to generate ROSs, such as H_2O_2, from the exited electrons when absorbing visible light.

The resultant MIC, 4.17 ppm, was less than half of that of commercial AgNPs (10 ppm) as reported by Li et al. [5]. In addition, the synthesis was one-step and green, which indicated that the NPs are a better option economically.

2022 S.-T. Yau High School Science Award
仅用于2022丘成桐中学科学奖公示

Although the Chitosan/AgNPs precipitated out in this test, its outstanding performance in the disc-diffusion method should not be overlooked. It is proposed that the OD_{600} analysis could be modified by adding pH buffer to obtain a suitable pH for both Chitosan/AgNPs and the growth of E. coli.

Furthermore, gram-positive bacteria, such as Staphylococcus aureus, should also be used as a bacterial model in future studies, to obtain a more accurate MIC of AgNPs for general sterilization purposes.

7 Antifungal activity test

7.1 Experimental

7.1.1.1 Materials

The fungi solution was prepared by scraping the mold from a moldy mango seed and putting it into distilled water followed by shaking and sonication. Squared bread was purchased from A1 bakery.

7.1.1.2 Antifungal activity test using bread as the culture medium

Starch/, Alginate, Chitosan, Okra-0.25% and Okra-0.5%/AgNPs were tested for their anti-fungal effects.

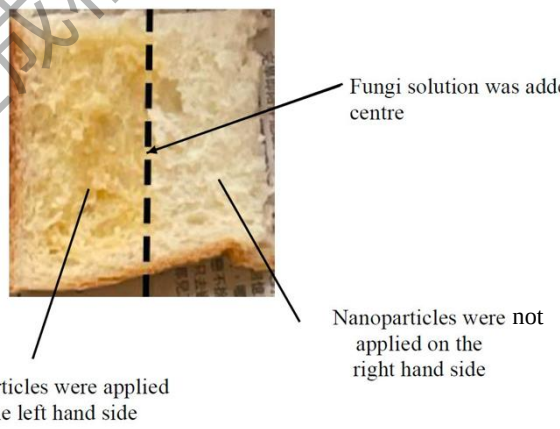

Figure 22: the method of applying AgNPs and fungi onto a bread.

First, each slice of bread was cut into 4 equal squares. 2 set-ups were prepared as follows: the first set was prepared by adding 1 drop of the fungi solution at the center of the bread and spreading it with a brush, followed by the addition and spreading of 1 mL of NPs of various capping agents and concentrations (100/50/25/10/5/2.5/1/0 (background) ppm) on the left-hand side of the slices of bread.

2022 S.T. Yau High School Science Award
仅用于2022丘成桐中学科学奖公示

The second set was prepared by reversing the sequence of addition mentioned above. The above samples were put into plastic bags and placed under room conditions with the humidity at around 80% for 1 week. The anti-fungal effect of each type and concentration of the NPs was determined by the number of days taken for the fungi to contaminate the left-hand side of each slice of bread.

7.2 Result

In general, for the first 3 days, there was no observable change on all samples. The development of the mold could be observed starting from the 4th day. The samples with 100 ppm NPs solutions lasted longer before the left-hand sides were contaminated with mold.

Picture 30: conducting antifungal activity test

2022 S.-T. Yau High School Science Award
仅用于2022丘成桐中学科学奖公示

7.2.1 Starch/AgNPs

7.2.1.1 The first set (fungi added first)

In Table 5, fungal contamination was first observed on the 4th day, in concentrations of 0, 1, 2.5, 5, 10 and 25 ppm (highlighted in yellow). For the concentration of 50 ppm and 100 ppm, fungal contamination was observed on the 5th (highlighted in blue) and 6th (highlighted in green) day respectively.

7								
6								
5							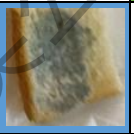	
4								
3					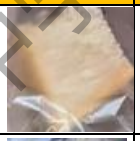	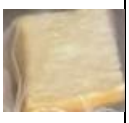		
2								
1								
Day/Conc.	0 ppm	1 ppm	2.5 ppm	5 ppm	10 ppm	25 ppm	50 ppm	100 ppm

Table 5: the result of Starch/AgNPs (first set) in the antifungal test.

2022 S.T. Yau High School Science Award
仅用于2022丘成桐中学科学奖评审

7.2.1.2 The second set (AgNPs added first)

In Table 6, fungal contamination was first observed on the 4th day, in concentrations of 0, 1, 2.5, 5, 10 and 25 ppm (highlighted in yellow). For the concentration of 50 ppm and 100 ppm, fungal contamination was observed on the 5th (highlighted in blue) and 6th (highlighted in green) day respectively.

7						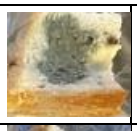	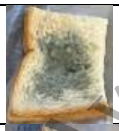	
6					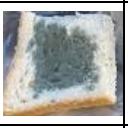		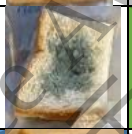	
5								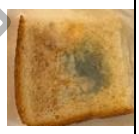
4				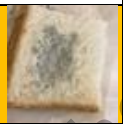	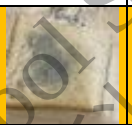			
3								
2								
1								
Day/conc.	0 ppm	1 ppm	2.5 ppm	5 ppm	10 ppm	25 ppm	50 ppm	100 ppm

Table 6: the result of Starch/AgNPs (second set) in the antifungal test.

Figure 23: the result of both sets of Starch/AgNPs in the antifungal test.

2022 S.T.Yau High School Science Award
仅用于2022丘成桐中学科学奖

7.2.2 Alginate/AgNPs

7.2.2.1 The first set (fungi added first)

In Table 7, fungal contamination was first observed on the 4th day, in concentrations of 0, 1, 2.5, 5, 10 and 25 ppm (highlighted in yellow). For the concentration of 50 ppm and 100 ppm, fungal contamination was observed on the 5th (highlighted in blue) and 6th (highlighted in green) day respectively.

7								
6						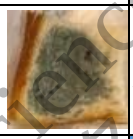	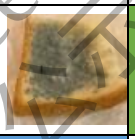	
5					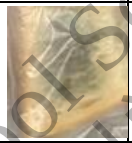	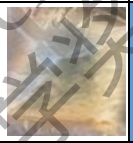		
4								
3								
2								
1								
Day/conc.	0 ppm	1 ppm	2.5 ppm	5 ppm	10 ppm	25 ppm	50 ppm	100 ppm

Table 7: the result of Alginate/AgNPs (first set) in the antifungal test.

2022 S.-T. Yau High School Science Award
仅用于2022丘成桐中学科学奖公开

7.2.2.2 The second set (AgNPs added first)

In Table 8, fungal contamination was first observed on the 4th day, in concentrations of 0, 1, 2.5, 5, 10, 25 and 50 ppm (highlighted in yellow). For the concentration of 100 ppm, fungal contamination was observed on the 6th day (highlighted in blue).

Day/Conc.	0 ppm	1 ppm	2.5 ppm	5 ppm	10 ppm	25 ppm	50 ppm	100 ppm
7						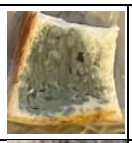		
6								
5		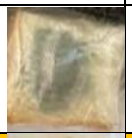			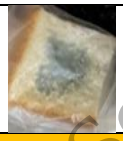			
4								
3	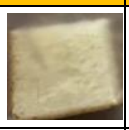							
2								
1								

Table 8: the result of Alginate/AgNPs (second set) in the antifungal test.

Figure 24: the result of both sets of Alginate/AgNPs in the antifungal test.

2022 S.T.Yau High School Science Award
仅用于2022丘成桐中学科学奖

7.2.3 Chitosan/AgNPs

7.2.3.1 The first set (fungi added first)

In Table 9, fungal contamination was first observed on the 4th day, in concentrations of 0, 1, 2.5, 5, 10 and 25 ppm (highlighted in yellow). For the concentration of 50 ppm and 100 ppm, fungal contamination was observed on the 6th (highlighted in blue) and 7th (highlighted in green) day respectively.

Day/Conc.	0 ppm	1 ppm	2.5 ppm	5 ppm	10 ppm	25 ppm	50 ppm	100 ppm
7								
6								
5				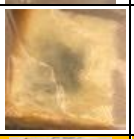				
4								
3								
2								
1								

Table 9: the result of Chitosan/AgNPs (first set) in the antifungal test.

2022 S.T. Yau High School Science Award
仅用于2022丘成桐中学科学奖

7.2.3.2 The second set (AgNPs added first)

In Table 10, fungal contamination was first observed on the 4th day, in concentrations of 0, 1, 2.5, 5, 10 and 25 ppm (highlighted in yellow). For the concentration of 50 ppm and 100 ppm, fungal contamination was observed on the 6th (highlighted in blue) and 7th (highlighted in green) day respectively.

7	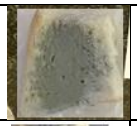							
6								
5								
4								
3								
2								
1								
Day/Conc.	0 ppm	1 ppm	2.5 ppm	5 ppm	10 ppm	25 ppm	50 ppm	100 ppm

Table 10: the result of Chitosan/AgNPs (second set) in the antifungal test.

Figure 25: the result of both sets of Chitosan/AgNPs in the antifungal test.

2022 S.-T. Yau High School Science Award
仅用于2022丘成桐中学科学奖

7.2.4 Okra-0.25%/AgNPs

7.2.4.1 The first set (fungi added first)

In Table 11, fungal contamination was first observed on the 4th day, in concentrations of 0, 1, 2.5, 5, 10 and 25 ppm (highlighted in yellow). For the concentration of 50 ppm and 100 ppm, fungal contamination was observed on the 5th (highlighted in blue) and 6th (highlighted in green) day respectively.

7								
6					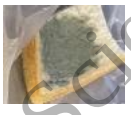			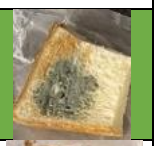
5					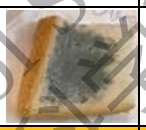			
4								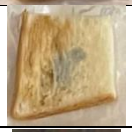
3		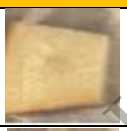						
2								
1								
Day/Conc.	0 ppm	1 ppm	2.5 ppm	5 ppm	10 ppm	25 ppm	50 ppm	100 ppm

Table 11: the result of Okra-0.25%/AgNPs (first set) in the antifungal test.

2022 S.T.Yau High School Science Award
仅用于2022丘成桐中学科学奖

7.2.4.2 The second set (AgNPs added first)

In Table 12, fungal contamination was first observed on the 4th day, in concentrations of 0, 1, 2.5, 5, 10 and 25 ppm (highlighted in yellow). For the concentration of 50 ppm and 100 ppm, fungal contamination was observed on the 5th (highlighted in blue) and 6th (highlighted in green) day respectively.

7								
6								
5								
4							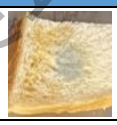	
3	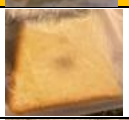							
2								
1								
Day/Conc.	0 ppm	1 ppm	2.5 ppm	5 ppm	10 ppm	25 ppm	50 ppm	100 ppm

Table 12: the result of Okra-0.25%/AgNPs (second set) in the antifungal test.

Figure 26: the result of both sets of Okra-0.25%/AgNPs in the antifungal test.

2022 S.-T. Yau High School Science Award
仅用于2022丘成桐中学科学奖

7.2.5 Okra-0.5%/AgNPs

7.2.5.1 The first set (fungi added first)

In Table 13, fungal contamination was first observed on the 4th day, in concentrations of 0, 1, 2.5, 5 and 10 ppm (highlighted in yellow). For the concentration of 25, 50 ppm and 100 ppm, fungal contamination was observed on the 5th day (highlighted in blue).

7								
6					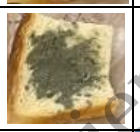			
5			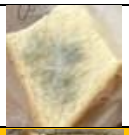	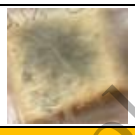				
4								
3								
2								
1								
Day/Conc.	0 ppm	1 ppm	2.5 ppm	5 ppm	10 ppm	25 ppm	50 ppm	100 ppm

Table 13: the result of Okra-0.5%/AgNPs (first set) in the antifungal test.

2022 S.T. Yau High School Science Award
仅用于2022丘成桐中学科学奖公示

7.2.5.2 The second set (AgNPs added first)

In Table 14, fungal contamination was first observed on the 4th day, in concentrations of 0, 1, 2.5, 5, 10 and 25 ppm (highlighted in yellow). For the concentration of 50 ppm and 100 ppm, fungal contamination was observed on the 5th day (highlighted in blue).

7							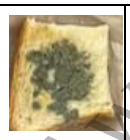	
6								
5	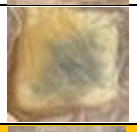	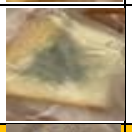						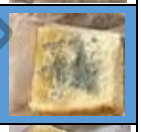
4								
3								
2								
1								
Day/Conc.	0 ppm	1 ppm	2.5 ppm	5 ppm	10 ppm	25 ppm	50 ppm	100 ppm

Table 14: the result of Okra-0.5%/AgNPs (second set) in the antifungal test.

Figure 27: the result of both sets of Okra-0.5%/AgNPs in the antifungal test.

2022 S.T.Yau High School Science Award
仅用于2022丘成桐中学科学奖

7.3 Discussion

The anti-fungal effect could be due to the fact that the nanoparticles could damage, penetrate, or destroy the cell membrane of the fungi. They could also release metal ions to bind with essential membrane proteins and affect their functions, disrupting electron transport. These would damage and eventually kill the fungi, thus inhibiting fungal growth. The 2 set-ups of different addition sequences showed slightly different results within the same kind of NPs. In general, the set-ups that added NPs before fungi showed slightly weaker anti-fungi effect. A possible explanation for this could be that the starch of the bread chelated the AgNPs directly, thus immobilized and deactivated the poisoning effect to the mold. At the same time, it was concluded that the Chitosan/AgNPs exhibited the strongest antifungal properties, followed by those of starch and alginate, 0.25% okra seed and then 0.5% okra seed.

The number of days needed for the fungi to contaminate the left-hand side (NPs-containing side) increased with the concentration of the NPs. This indicated that the greater the concentration of NPs, the smaller the degree of growth of the fungi. Moreover, 100 ppm NPs showed a significantly stronger effect on the inhibition of growth of the fungi (usually up to 6-7 days). The AgNPs entered the cell membrane and affected the respiratory chain seriously, resulting in cell death. Thus, it is believed that to suppress the growth of fungi using NPs, a concentration greater or equal to 100 ppm is needed.

2022 S.-T. Yau High School Science Award
仅用于2022丘成桐中学科学奖公示

8 AgNPs-hydrogel composite

8.1 Experimental

8.1.1 Materials

Polyvinyl alcohol (PVA) prepared from Rise Liquid Glue without purification, sodium tetraborate powder (purchased from UNI-CHEM).

8.1.2 Synthesis of the Nanoparticle-consisting PVA hydrogels

First, 20 mL of glue was added into each beaker followed by 3.34/1.66/0.84/0.34 mL of 100 ppm Starch/AgNPs solution to obtain hydrogels with the final concentrations of 16.7/8.3/4.2/1.7 ppm of AgNPs respectively. Then, the mixture was stirred quickly with a glass rod. Next, 0.1905 g of sodium tetraborate was dissolved in 5 mL of distilled water to obtain a saturated solution (~0.1 M), and then 0.2/0.5/1 mL of the saturated borax solution were added to the 3 sets of glues with 1.66/0.84/0.34 mL of AgNPs solution respectively. The mixtures were stirred with a glass rod during the addition. The above steps were repeated for Alginate/AgNPs and Chitson/AgNPs.

8.2 Result

The mixtures of PVA and AgNPs that turned into non-sticky gelatinous substances with an even distribution of the colour of the AgNPs solution (yellow) indicated the ideal formation of hydrogels (Pictures 31 and 32). However, it was observed that the less the amount of NPs solution added, the lower the mechanical strength of the hydrogels, and some sets of the hydrogels remained glue-like. The mixtures with 1.66/0.84/0.34mL AgNPs solution failed to form ideal hydrogels, hence the addition of sodium tetraborate, a chemical known to exhibit crosslinking effects. After the addition, ideal hydrogels were formed for the mixtures containing 1.66/0.84/0.34 mL of AgNPs solution as well.

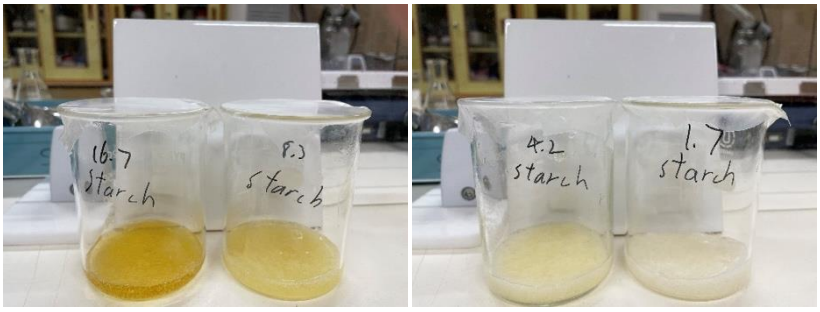

Picture 31: hydrogels made of Starch/AgNPs, from left to right: 16.7 ppm, 8.3 ppm, 4.2 ppm, 1.7 ppm.

2022 S.T.Yau High School Science Award
仅用于2022区域初中学科学术公示

For Starch/, Alginate/ and Chitosan/AgNPs-hydrogel composite, non-sticky gelatinous hydrated hydrogels were obtained. They were also elastic and flexible. Their colour density decreased with the concentration of AgNPs solution added, from orange to very pale yellow, as the NPs were the only dye present. It was also observed that the lower the amount of NPs solution added, the lower the mechanical strength of the hydrogels.

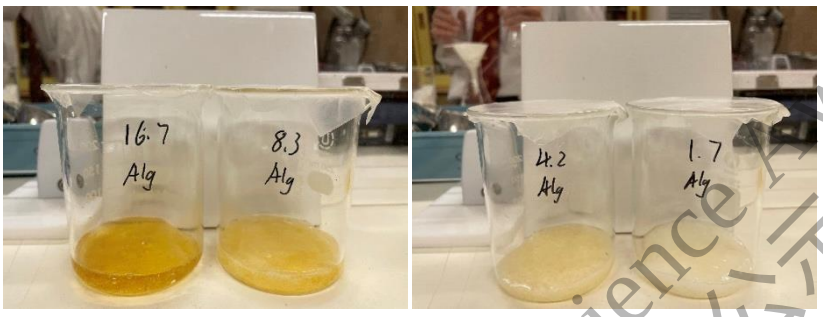

Picture 32: hydrogels made of Alginate/AgNPs, from left to right: 16.7 ppm, 8.3 ppm, 4.2 ppm, 1.7 ppm.

8.3 Discussion

8.3.1 Possible mechanisms of crosslinking

8.3.1.1 Hydrogen bond between capping agent and PVA

The crosslinking of the functionalized NPs could be explained by the chemical property of their capping agents. Both starch and alginate molecules consist of hydroxyl groups as functional groups. The functionalized NPs are like tiny spherical substances carrying multiple hydroxyl groups on their surface. When mixed with PVA, the hydroxyls group between NPs and PVA interact to from strong hydrogen bonds which results in gelation [23] (Figure 28).

2022 S.-T. Yau High School Science Award
仅用于2022丘成桐中学科学奖公示

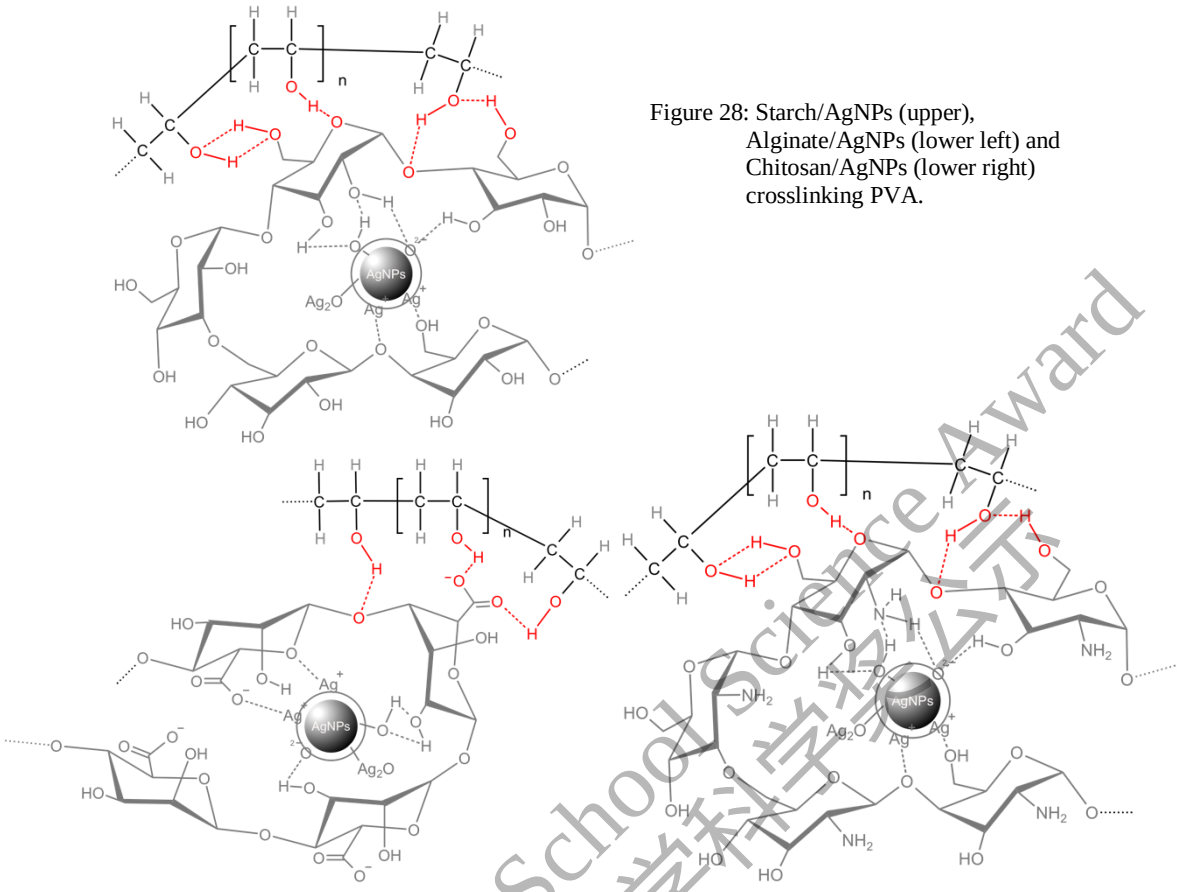

Figure 28: Starch/AgNPs (upper), Alginate/AgNPs (lower left) and Chitosan/AgNPs (lower right) crosslinking PVA.

8.3.1.2 Alkaline self-hydrolysis of sodium borohydride residue

Since excess sodium borohydride was used during the synthesis of Starch/, Alginate/ and Chitason/AgNPs, the remaining sodium borohydride underwent self-hydrolysis in the solution to form borate ions, $B(OH)_4^-$. First, the sodium borohydride dissociated in water. The BH_4^+ formed reacted with the hydroxide ions to form BH_3 which then slowly hydrolyzed to form boric acid and hydrogen in water. Finally, boric acid reacted with water to form borate ions that crosslinked PVA chains. The crosslinking effect would be explained in 8.3.1.3. The following equations (Equation 6) illustrate the above process [28].

Equation 6

General hydrolysis	$NaBH_4 + 4\,H_2O$	$\longrightarrow$	$NaB(OH)_4 + 4\,H_2$
Borane formation	$BH_4^- + H_2O$	$\longrightarrow$	$BH_3 + H_2 + OH^-$
Formation of borate ion	$BH_3 + 3\,H_2O + OH^-$	$\longrightarrow$	$B(OH)_4^- + 3\,H_2$
Dissociation of sodium tetraborate	$Na_2B_4O_7 + 7\,H_2O$	$\longrightarrow$	$2\,NaB(OH)_4 + 2\,B(OH)_3$

2022 S.-T. Yau High School Science Award
仅用于2022丘成桐中学科学奖公开

8.3.1.3 Addition of sodium tetraborate solution

As mentioned above, the saturated borax solution was added to the hydrogels with 8.3/4.2/1.7 ppm of AgNPs to increase the number of crosslinking points in order to form ideal hydrogels.

Figure 29: borate ion crosslinking

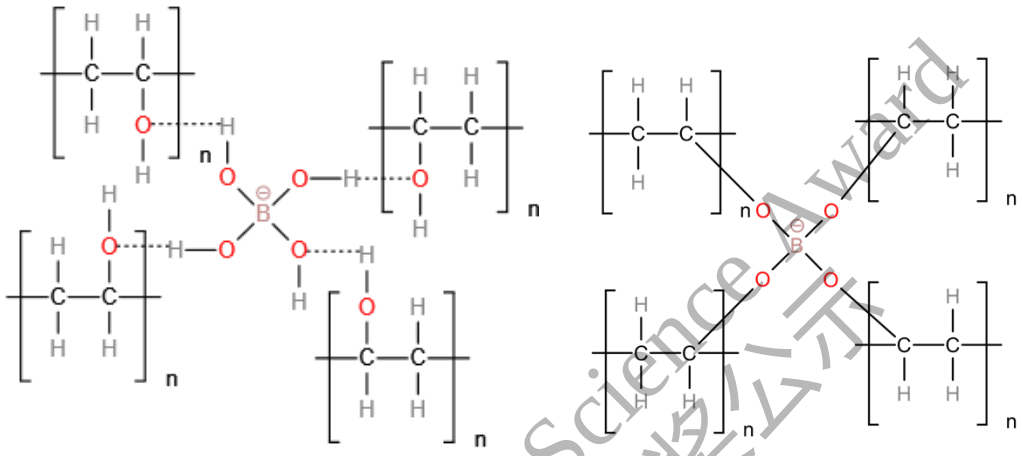

All four of the hydroxyl groups of borate ions, $B(OH)_4^-$, formed strong hydrogen bonds with the hydroxyl groups of PVA (Figure 29), resulting in similar crosslinking effect as that of functionalized NPs [29]. These hydrogen bonds were strong and dynamic, they were constantly forming and dissociating with the crosslinks moving randomly among the PVA molecules, contributing to the elasticity of hydrogel made.

8.3.1.4 Dative covalent bond between sliver ions and PVA

Since the NPs used were in solution form, with the presence of moisture, a layer of Ag_2O formed on the surface of AgNPs. The lone pair electrons of hydroxyl group of PVA displaced the oxide out from Ag_2O, contributing to the presence of silver ions and oxide ions. Then, the hydroxyl groups of PVA directly chelated the positive silver ions by dative covalent bond, resulting in the crosslinking of PVA chains (Equation 7).

Equation 7

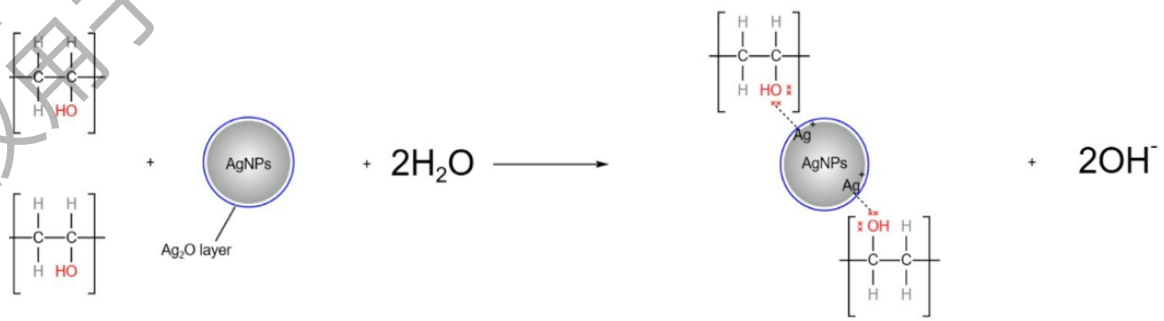

2022 S.T. Yau High School Science Award
仅用于2022丘成桐中学科学奖公开

8.3.2 Mechanical strength

When more crosslinkers were added, it increased the points where the polymer chains could entangle, resulting in a tighter and stiffer polymer material. This was believed to be the reason why hydrogels with poor mechanical strength were obtained when low concentrations of NPs were added. On the other hand, the crosslinking tended to link PVA molecules together in a way that they were no longer free to slide past one another. The large PVA molecules in the glue already could not move past each other easily, thus with the aid of the functionalized NPs and borate ions linking the big molecules to one another, forming even larger molecules, it became even more difficult for them to slide past one another. The result was a tangled mass. When applying a certain force to the hydrogel, it breaks some of the hydrogen bonds and allows the polymers to flow past each other more easily. When the force is removed, the hydrogen bonds between the polymer chains form again. This explains the outstanding flexibility of hydrogels made.

9 Detection of Cysteine by AgNPs

9.1 Experimental

9.1.1 Materials

Cysteine solution was prepared by dissolving solid cysteine in a pH10 buffer solution. The solution was then serial diluted to 1, 5, 10, 20, 40, 60, 80 and 100 ppm.

9.1.2 Interaction of cysteine with Starch/AgNPs

To investigate colour changes due to the interaction between cysteine and Starch/AgNPs, 0.2 mL of cysteine solution of contractions at 1, 5, 10, 20, 40, 60, 80 and 100 ppm were added with 0.1 mL of 100 ppm Starch/AgNPs into a spot plate respectively. Colour changes were observed and compared.

9.1.3 Interaction of cysteine with Alginate/AgNPs

The above procedures were repeated by using Alginate/AgNPs.

9.2 Results

It is observed that, at low concentrations (1 - 10 ppm) of cysteine, the colour changes were not visually observable. However, it is observed that the higher the concentration of cysteine (where [cysteine] ≥ 20 ppm), the darker the colour.

2022 S.-T. Yau High School Science Award
仅用于2022丘成桐中学科学奖公开

Besides, at [cysteine] = 20 ppm, the colour of Starch/AgNPs changes directly from yellow to red but that of Alginate/AgNPs changes from yellow to orange.

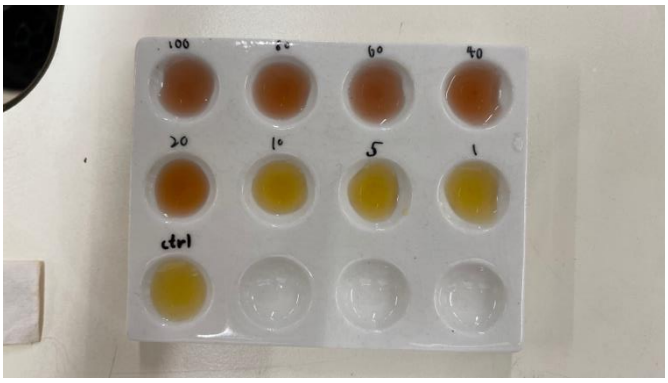

Picture 46: the changes in colour of cysteine added with Starch/AgNPs. From top to bottom, left to right: 100, 80, 60, 40, 20, 10, 5, 1 ppm.

Picture 47: the changes in colour of cysteine added with Alginate/AgNPs. From top to bottom, left to right: 100, 80, 60, 40, 20, 10, 5, 1 ppm.

9.3 Discussion

The changes in the absorbance and colour indicated the interaction between AgNPs and cysteine. It is proposed that under high pH, the carboxyl group of the cysteine molecule is deprotonated and the whole molecule becomes soluble. As the thiol group of cysteine forms strong chelation with silver, a cysteine-AgNPs complex is formed.

The colour of the mixture of cysteine and AgNPs changed drastically at 20 ppm, which corresponds to the threshold for proteinuria diagnosis (18.8 ppm). This method has a high potential for identifying patients suffering from proteinuria. Our implementation involves only a simple colour change from yellow to orange, or yellow to red, which can be easily measured and allows instant detection of the symptom.

10 Conclusion

Chitosan, alginate, okra, cysteine and starch-chelated AgNPs were successfully produced by one-step synthesis. Among these samples, the okra extract could be used as both the capping and reducing agents, without the addition of $NaBH_4$, providing a green synthesis pathway of AgNPs. However, the synthesized CuNPs were very unstable and oxidized quickly by reacting with the oxygen dissolved in the solution. They were also unsuitable for the application onto hydrogels.

The antibacterial effect of Chitosan/AgNPs was the strongest, followed by Starch/ and Alginate/AgNPs. The antibacterial effect of Okra/AgNPs was not significant, due to their polydispersity of diameters. The MIC of Starch/AgNPs and

2022 S.T. Yau High School Science Award
仅用于2022丘成桐中学科学奖公示

Alginate/AgNPs are 4.17 ppm, which was less than half of that of the commercial one. However, a relatively low antifungal effect was observed in AgNPs, in which a notable delay in fungal growth was only presented in AgNPs with a concentration of 100 ppm. It is concluded that the synthesized AgNPs can be used to prevent bacterial infection, but cannot prevent fungal infection just as effectively.

Hydrogels were successfully made from our Starch/, Alginate/ and Chitosan/AgNPs and multiple possible crosslinking mechanisms were suggested. This enhances the potential of the application of our synthesized AgNPs towards wound treatment.

11 Future work

AgNPs were successfully synthesized from okra extracts, which is a novel capping and reducing agent. However, the diameter of the synthesized AgNPs has shown a polydispersity pattern as mentioned in section 5.2.1.4, resulting in a decreased antibacterial and antifungal effect. Hence, further experiments such as purification and infrared spectroscopy analysis should be carried out to determine the functional chemicals that contribute to its capping-reducing capability.

From the result of the antibacterial test, it is deduced that the antibacterial activity of the synthesized AgNPs may not be catalytic. Hence, it is hypothesized that dye-sensitized AgNPs may be more effective against bacteria in the exposure of visible light (see section 0). Further research could be done to synthesize dye-sensitized AgNPs.

Physical properties such as the degree of swelling, water retention capacity and water vapor transmission rate of the hydrogels should be tested, to determine whether they are the ideal wound dressing mentioned in the introduction. Mechanism 8.3.1.2 and 8.3.1.3 were believed to be more possible since the crosslinking effect of borate ions are well-known. Besides, further control set-ups should be designed to verify the mechanisms. For example, adding pure capping agent solution into PVA to see whether hydrogel can also be formed, and using NPs reduced by reducing agents other than sodium borohydride to synthesize the hydrogels.

2022 S.-T. Yau High School Science Award
仅用于2022丘成桐中学科学奖公示

12 Appendix – More to Synthesis of nanoparticles

12.1 Experimental

12.1.1 Materials

12.1.1.1 Green tea

To obtain a green tea extract, 4 g of green tea leaves were added to 200 mL of distilled water and stirred for 30 minutes. Then, the tea leaves were removed from the mixture using a sieve. The mixture was filtered, such that the soluble substances were retained.

12.1.1.2 Aloe vera

To obtain an aloe vera extract, the inner leaf of the aloe vera was removed from the plant and put into a blender with distilled water. After blending, the mixture was centrifuged to remove insoluble substances.

Picture 33: removal of the inner leaf of the aloe vera plant

12.1.1.3 Avocado seed

To obtain an extract of the avocado seeds, they were blended into fine powders and then dissolved in distilled water. The mixture was then filtered such that the soluble substances are retained. The concentration of the solution was then measured.

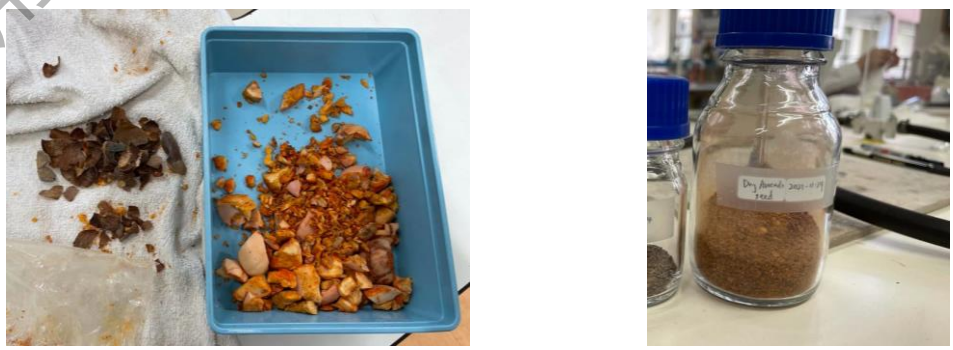

Picture 34: avocado seeds blended into powders

2022 S.-T. Yau High School Science Award
仅用于2022丘成桐中学科学奖公示

12.1.2 Silver nanoparticles

12.1.2.1 Tea extract

To synthesize tea extract-chelated AgNPs, 50 mL of 2% tea extract solution was prepared with the addition of 3 mL of 4000 ppm NaOH solution, such that it had a pH value of 8. 2 mL of 5000 ppm $AgNO_3$ solution was added to 48 mL of water. Then, the tea extract was added dropwise to the silver ion solution with stirring. The above procedures were repeated by adding the silver ion solution dropwise to the tea extract solution with stirring.

12.1.2.2 Aloe vera extract

To synthesize aloe vera-chelated AgNPs, 5 mL and 10 mL of the aloe vera extract were made up to 50 mL respectively. 2 mL of the 5000 ppm $AgNO_3$ solution was added to 48 mL of distilled water. Then, the silver ion solution was added dropwise to the 2 sets of aloe vera extract solution respectively at room temperature with stirring.

12.1.2.3 Avocado seed

To synthesize avocado seed-chelated AgNPs, 3 sets of 50 mL avocado seed extract solution containing 5 mL of 10% ammonia solution were prepared, such that they contained 4 g, 1 g and 0.5 g of the seed extract respectively. 2 mL of the 5000 ppm $AgNO_3$ solution was added to 48 mL of distilled water. Then, the silver ion solution was added dropwise to the solution of avocado seed extract at room temperature with stirring.

12.1.2.4 L-ascorbic acid

To synthesize L-ascorbic acid-chelated AgNPs, 0.033 g of L-ascorbic acid was dissolved in 44 mL distilled water. 6 mL of pH10 buffer solution was added. 2 mL of the 5000 ppm $AgNO_3$ solution was added to 48 mL of distilled water. The mole ratio of Ag^+:L-ascorbic acid was 1:2. Then, the solution of L-ascorbic acid was added dropwise to the silver ion solution at 80°C with stirring.

12.1.2.5 Cysteine

To synthesize cysteine-chelated AgNPs, 0.004 g and 0.003 g of cysteine was added to 48 mL of distilled water. 2 mL of the 5000 ppm $AgNO_3$ solution was added to the cysteine solution, such that the mole ratio of Ag^+:cysteine was 3:1 and 4:1 respectively. To dissolve the cysteine, the solution was sonicated for 15 minutes and

2022 S.T.Yau High School Science Award
仅用于2022丘成桐中学科学奖公示

then heated by the Bunsen burner with a non-luminous flame for 10 minutes. Then, 0.105 g of $NaBH_4$ was added to 50 mL of distilled water in an ice bath. The mole ratio of Ag^+:$NaBH_4$ was 1:30, such that the reducing agent was in excess. Then, the cysteine-chelated silver ion solution was added dropwise to the $NaBH_4$ solution in the ice bath with stirring.

12.1.3 Copper nanoparticles

12.1.3.1 Cysteine

To synthesize cysteine-chelated CuNPs, various trials were carried out. Using $NaBH_4$ as the reducing agent, 0.178 g of $NaBH_4$ was added to 50 mL of distilled water in an ice bath. The mole ratio of Cu^{2+}:$NaBH_4$ is 1:30, such that the reducing agent was in excess. 0.004 g of cysteine was added into 48 mL of distilled water. Then, 2 mL of 5000 ppm $CuCl_2$ was added to the cysteine solution, such that the mole ratio between cysteine and copper(II) ions was 1:5. To dissolve the cysteine, the solution was sonicated for 15 minutes and then heated by the Bunsen burner with a non-luminous flame for 10 minutes. After that, the cysteine-chelated copper(II) ion solution was made up to 50 mL and added dropwise to the $NaBH_4$ solution in the ice bath with stirring.

Using L-ascorbic acid as the reducing agent, 0.832 g of L-ascorbic acid was dissolved in 50 mL of distilled water. The mole ratio of Cu^{2+}:L-ascorbic acid was 1:30, such that the reducing agent was in excess. 0.006 g and 0.005 g of cysteine were added to 48 mL of distilled water respectively. Then, for each cysteine solution, 2 mL of 5000 ppm $CuCl_2$ was added to the cysteine solution, such that the mole ratio of cysteine and copper(II) ions were 1:3 and 1:4. To dissolve the cysteine, the solution was sonicated for 15 minutes and then heated by the Bunsen burner with a non-luminous flame for 10 minutes. After that, the cysteine-chelated copper(II) ion solution was made up to 50 mL and heated to 80°C. After that, the solution of L-ascorbic acid was added dropwise to the cysteine-chelated copper(II) ion solution at 80°C with stirring.

Using glucose as the reducing agent. 0.631 g of NaOH was dissolved in 50 mL of distilled water that gave the solution a pH value of 12. Then, 0.038 g cysteine was dissolved in the solution. After that, 2.835 g of glucose was dissolved in the alkaline cysteine solution. 2 mL of the 5000 ppm $CuCl_2$ solution was added to 48 mL of distilled water, such that the mole ratio of Cu^{2+}:Cysteine:Glucose:NaOH was

2022 S.T.Yau High School Science Award
仅用于2022丘成桐中学科学奖公示

1:2:100:100. The copper(II) ion solution was then added dropwise to the alkaline cysteine-glucose solution with stirring.

12.1.3.2 Tea extract

To synthesize tea extract-chelated CuNPs, 50 mL of 2% tea extract solution was prepared. 2 mL of 5000 ppm $CuCl_2$ was added to 48 mL of water. Then, the solution of tea extract was added dropwise to the copper(II) ion solution with stirring. The above procedures were repeated by adding the copper(II) ion solution dropwise to the solution of tea extract. After the additions were completed, the resultant solutions were heated at 80°C for 1.5 hours.

12.1.3.3 Aloe vera extract

To synthesize aloe vera-reduced-and-chelated CuNPs, 5 mL and 10 mL of the aloe vera extract were made up to 50 mL respectively. 2 mL of the 5000 ppm $CuCl_2$ solution was added to 48 mL of distilled water. Then, the copper(II) ion solution was added dropwise to the 2 sets of aloe vera extract solution respectively at room temperature with stirring.

To synthesize aloe vera-chelated CuNPs reduced by sodium borohydride, 5 mL and 10 mL of the aloe vera extract were made up to 48 mL respectively. 2 mL of 5000 ppm $CuCl_2$ was added to the 2 sets of aloe vera extract solution respectively. 0.178 g of $NaBH_4$ was dissolved in 50 mL of ice-bathed distilled water. The mole ratio of Cu^{2+}:$NaBH_4$ was 1:30, such that the reducing agent was in excess. The aloe vera-chelated copper(II) ion solution was added dropwise to the ice-bathed $NaBH_4$ solution with stirring.

2022 S.-T. Yau High School Science Award
仅用于2022丘成桐中学科学奖公示

12.2 Results

12.2.1 Silver nanoparticles

12.2.1.1 Tea extract

Using a tea extract as both the capping agent and the reducing agent produced an unclear solution of greyish brown colour with precipitates (Picture 35).

Picture 35: product of Ag capped and reduced by 1% tea extract.

12.2.1.2 Aloe vera extract

When using an aloe vera extract as both the capping agent and the reducing agent, the set-ups had no colour change initially. Upon heating, the set-up with a 5% volume ratio of the extract developed a light reddish colour, producing a clear solution with precipitates of a reddish-brown colour, while the set-up with a 10% volume ratio of the extract developed a light brownish colour, producing a clear solution with precipitates of a yellowish-brown colour (Picture 36).

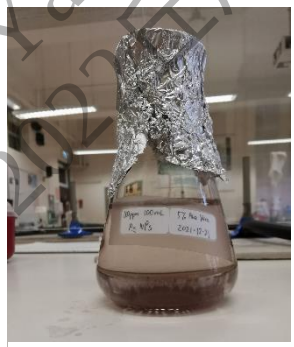

Picture 36: Left: Ag with 5% aloe vera extract (capping and reducing agent); Right: Ag with 10% aloe vera extract (capping and reducing agent).

2022 S.T. Yau High School Science Award
仅用于2022年丘成桐中学科学奖公示

12.2.1.3 Avocado seed

When using different concentrations of the extract of avocado seed, all 3 set-ups produced clear solutions with no precipitates. The set-ups of 0.5%, 1% and 4% of the extract were of pale yellow, yellow and light brown colours respectively (Picture 37).

Picture 37:

Left: Ag with 4% avocado seed extract (capping and reducing agent);

Middle: Ag with 0.5% avocado seed extract (capping and reducing agent);

Right: Ag with 1% avocado seed extract (capping and reducing agent)

12.2.1.4 L-ascorbic acid

Using L-ascorbic acid as both the capping agent and the reducing agent, the solution obtained was unclear and yellowish-white in colour, with precipitates (Picture 38).

Picture 38: Ag with L-ascorbic acid (capping and reducing agent).

2022 S.-T. Yau High School Science Award
仅用于2022丘成桐中学科学奖公开赛

12.2.1.5 Cysteine

Using different concentrations of cysteine as a capping agent and sodium borohydride as a reducing agent, a clear and dark wine-reddish solution of silver nanoparticles with no precipitates could be obtained (Picture 39).


Picture 39: Left: Ag with cysteine (capping agent) (Ag^+:cysteine=4:1) and sodium borohydride (reducing agent);
Right: Ag with cysteine (capping agent) (Ag^+:cysteine=3:1) and sodium borohydride (reducing agent).

12.2.2 Copper nanoparticles

12.2.2.1 Cysteine

Using cysteine as the capping agent and sodium borohydride as the reducing agent, an unclear black solution was obtained (Picture 40).

Picture 40: Cu with cysteine (capping agent) and sodium borohydride (reducing agent).

Using cysteine as the capping agent and L-ascorbic acid as the reducing agent, the set-ups with copper(II) ions:cysteine equal to 3:1 and 4:1 added both appeared to be unclear and in light yellow colour. After 9 hours of constant stirring and heating, both of the solutions remained unclear and they were of pale yellow and orange colour respectively (Picture 42).

2022 S.-T. Yau High School Science Award
仅用于2022丘成桐中学科学奖公示

Using cysteine as the capping agent and glucose as the reducing agent, a clear wine-reddish solution with no precipitates was obtained. However, it was noted that before the addition of copper(II) ions, the solution with cysteine, sodium hydroxide and glucose already shows a wine red colour (Picture 41).

Picture 42:

Upper: Cu with cysteine (capping agent) (Cu^{2+}:cysteine=3:1) and L-ascorbic acid (reducing agent), before and after 9 hours of constant stirring and heating;

Lower: Cu with cysteine (capping agent) (Cu^{2+}:cysteine=4:1) and L-ascorbic acid (reducing agent), before and after 9 hours of constant stirring and heating.

Picture 41: Cu with cysteine (capping agent) and glucose (reducing agent), before and after addition of the copper ion solution.

2022 S.T. Yau High School Science Award
仅用于2022年成桐中学科学奖公示

12.2.2.2 Tea extract

Using tea extract as both the capping and reducing agent, both solutions, one with the tea extract added dropwise while the other with the copper(II) chloride solution added dropwise, appeared to be clear with brown precipitates. Clear brown solutions were obtained after centrifugation (Picture 43).

Picture 43:
Left: Cu with tea extract (capping and reducing agent), Cu^{2+} added dropwise;
Middle: Cu with tea extract (capping and reducing agent), tea extract added dropwise;
Right: Cu with tea extract (capping and reducing agent), Cu^{2+} added dropwise, after centrifugation.

12.2.2.3 Aloe vera extract

When using an aloe vera extract as both the capping agent and the reducing agent, the set-ups had no colour change initially. Upon heating, the set-up with a 5% volume ratio of the extract remained colourless, while the set-up with a 10% volume ratio of the extract developed a light pink colour, producing a clear solution with no precipitates (Picture 44).

Picture 44: Left: Cu with 5% aloe vera extract (capping and reducing agent);
Right: Cu with 10% aloe vera extract (capping and reducing agent).

2022 S.-T. Yau High School Science Award
仅用于2022丘成桐中学科学奖公示

When using aloe vera as the capping agent and $NaBH_4$ as the reducing agent, for both concentrations, 5% and 10%, unclear solutions in a black colour were observed after a few drops of aloe vera-chelated copper(II) ion solution had been added (Picture 45).

Picture 45: Left: Cu with 5% aloe vera extract (capping agent) and sodium borohydride (reducing agent); Right: Cu with 10% aloe vera extract (capping agent) and sodium borohydride (reducing agent).

12.3 Discussion

12.3.1 Silver nanoparticles

12.3.1.1 Tea extract

While using tea extract in the synthesis of silver nanoparticles, both with or without proven reliable capping agents including starch and chitosan, the reduced silver aggregated. It is believed that the tea extract itself act as a capping agent and bind with the silver ions, so while a low concentration of the tea extract is insufficient for the complete reduction of the silver ions, a high concentration will lead to the interconnection of the nanoparticles via hydrogen bonds between the capping agents, resulting in aggregation [30]. Therefore, tea extract is not an ideal reducing agent.

12.3.1.2 Aloe vera

The set-ups involving the aloe vera extracts had a pale colour with a large amount of precipitates. The pale colour indicated a small degree of reaction, so it is concluded that the aloe vera extract had a small reducing power even upon heating. The precipitates indicated that the aloe vera extract was also unable to chelate the silver ions and prevent aggregation, so it is neither a suitable reducing agent nor a suitable capping agent for the synthesis of silver nanoparticles.

12.3.1.3 Avocado seed extract

When the extract of an avocado seed was used as the capping agent and the reducing agent, the solutions produced were all clear with no precipitates, so the extract is a

2022 S.-T. Yau High School Science Award
仅用于2022正成利中学科学奖公示

suitable capping agent. However, the colours of all 3 set-ups were lighter than that of existing successful samples, which was probably due to the incomplete reduction of all silver ions. Thus, it is concluded that the extract does not have a strong enough reducing power.

12.3.1.4 L-ascorbic acid

The silver solution reduced by L-ascorbic acid was very unclear with many precipitates of silver metal. Therefore, while L-ascorbic acid is a strong enough reducing agent, it is unable to chelate the silver nanoparticles and prevent aggregation.

12.3.1.5 Cysteine

The combination of cysteine as a capping agent and sodium borohydride as a reducing agent produced silver nanoparticles successfully, but it was observed that the colour of the resultant solutions is much deeper than that of existing successful samples. This may be because only a small amount of cysteine can be dissolved and used to chelate the silver ions before reduction, so its capping capabilities are not as good as that of starch or alginate, leading to a slightly larger particle size.

12.3.2 Copper nanoparticles

12.3.2.1 Cysteine

Cysteine can also act as a capping agent. Yet, unclear solutions were observed when sodium borohydride or L-ascorbic acid were used as the reducing agents with cysteine as the capping agent. The aggregation of copper nanoparticles may be due to the insufficient amount of capping agents, leading to aggregation. Regarding the set-up with glucose as the reducing agent, it was noted that the solution containing cysteine, sodium hydroxide and glucose was wine red in colour both before and after the addition of copper precursors. Before the addition of copper(II) ions, the dehydration of glucose produced a wine red colour, while the successful formation of copper nanoparticles might also produce a wine red colour. As the colours would overlap, it was difficult to determine if copper nanoparticles had indeed formed.

12.3.2.2 Tea extract

Although clear solutions were obtained after the initially unclear brownish solutions with a tea extract as both the capping agent and reducing agent were centrifuged, no optical path was observed when being shone on by a laser pointer. This indicated the

2022 S.-T. Yau High School Science Award
仅用于2022丘成桐中学科学奖公示

absence of nanoparticles, and thus the tea extract is not suitable for the synthesis of copper nanoparticles because the precipitates are probably aggregated copper metal.

12.3.2.3 Aloe vera

There were no observable changes for the set-up using 5% aloe vera extract as both the reducing and capping agent while the one with 10% aloe vera extract showed a small change in colour. Therefore, there were no significant differences for the solutions before and after the addition of aloe vera extract, indicating that the reducing power of aloe vera is not strong enough to reduce the copper(II) ions.

For the set-ups using aloe vera as the capping agent and $NaBH_4$ as the reducing agent, the solution turned black and became unclear once a few drops of aloe vera-chelated copper(II) ion solution were added. This indicated the aggregation of copper and that aloe vera is not able to cap the CuNPs formed.

2022 S.-T. Yau High School Science Award
仅用于2022丘成桐中学科学奖公示

13 References

(1) Abou El-Nour, K. M. M.; Eftaiha, A.; Al-Warthan, A.; Ammar, R. A. A. Synthesis and Applications of Silver Nanoparticles. *Arabian Journal of Chemistry* **2010**, *3* (3), 135–140. https://doi.org/10.1016/j.arabjc.2010.04.008.

(2) Cheung, R.; Ng, T.; Wong, J.; Chan, W. Chitosan: An Update on Potential Biomedical and Pharmaceutical Applications. *Marine Drugs* **2015**, *13* (8), 5156–5186. https://doi.org/10.3390/md13085156.

(3) Dantas, T. L.; Alonso Buriti, F. C.; Florentino, E. R. Okra (Abelmoschus Esculentus L.) as a Potential Functional Food Source of Mucilage and Bioactive Compounds with Technological Applications and Health Benefits. *Plants* **2021**, *10* (8), 1683. https://doi.org/10.3390/plants10081683.

(4) Lee, K. Y.; Mooney, D. J. Alginate: Properties and Biomedical Applications. *Progress in Polymer Science* **2018**, *37* (1), 106–126. https://doi.org/10.1016/j.progpolymsci.2011.06.003.

(5) Li, W.-R.; Xie, X.-B.; Shi, Q.-S.; Zeng, H.-Y.; OU-Yang, Y.-S.; Chen, Y.-B. Antibacterial Activity and Mechanism of Silver Nanoparticles on Escherichia Coli. *Appl Microbiol Biotechnol* **2010**, *85* (4), 1115–1122. https://doi.org/10.1007/s00253-009-2159-5.

(6) Biyani, C. S.; Cartledge, J. J. Cystinuria—Diagnosis and Management. *EAU-EBU Update Series* **2006**, *4* (5), 175–183. https://doi.org/10.1016/j.eeus.2006.06.001.

(7) Rehman, T.; Shabbir, M. A.; Inam-Ur-Raheem, M.; Manzoor, M. F.; Ahmad, N.; Liu, Z.; Ahmad, M. H.; Siddeeg, A.; Abid, M.; Aadil, R. M. Cysteine and Homocysteine as Biomarker of Various Diseases. *Food Sci Nutr* **2020**, *8* (9), 4696–4707. https://doi.org/10.1002/fsn3.1818.

(8) Kalantari, K.; Mostafavi, E.; Afifi, A. M.; Izadiyan, Z.; Jahangirian, H.; Rafiee-Moghaddam, R.; Webster, T. J. Wound Dressings Functionalized with Silver Nanoparticles: Promises and Pitfalls. Nanoscale 2020, 12 (4), 2268–2291. https://doi.org/10.1039/C9NR08234D.

(9) Boonkaew, B.; Suwanpreuksa, P.; Cuttle, L.; Barber, P. M.; Supaphol, P. Hydrogels Containing Silver Nanoparticles for Burn Wounds Show Antimicrobial Activity without Cytotoxicity. *J. Appl. Polym. Sci.* **2014**, *131* (9), n/a-n/a. https://doi.org/10.1002/app.40215.

(10) Tian, J.; Wong, K. K. Y.; Ho, C.-M.; Lok, C.-N.; Yu, W.-Y.; Che, C.-M.; Chiu, J.-F.; Tam, P. K. H. Topical Delivery of Silver Nanoparticles Promotes Wound Healing. *ChemMedChem* **2007**, *2* (1), 129–136. https://doi.org/10.1002/cmdc.200600171.

(11) Yin, I. X.; Zhang, J.; Zhao, I. S.; Mei, M. L.; Li, Q.; Chu, C. H. The Antibacterial Mechanism of Silver Nanoparticles and Its Application in Dentistry. *Int. J. Nanomedicine* **2020**, *Volume 15*, 2555–2562. https://doi.org/10.2147/IJN.S246764.

(12) Ishida, T. Antibacterial Mechanism of Ag+ Ions for Bacteriolyses of Bacterial Cell Walls via Peptidoglycan Autolysins, and DNA Damages. *MOJ Toxicol.* **2018**, *4* (5). https://doi.org/10.15406/mojt.2018.04.00125.

(13) Liau, S. Y.; Read, D. C.; Pugh, W. J.; Furr, J. R.; Russell, A. D. Interaction of Silver Nitrate with Readily Identifiable Groups: Relationship to the Antibacterialaction of Silver Ions. *Lett. Appl. Microbiol.* **1997**, *25* (4), 279–283. https://doi.org/10.1046/j.1472-765X.1997.00219.x.

(14) Takahashi-Íñiguez, T.; Aburto-Rodríguez, N.; Vilchis-González, A. L.; Flores, M. E. Function, Kinetic Properties, Crystallization, and Regulation of Microbial Malate Dehydrogenase. *J. Zhejiang Univ.-Sci. B* **2016**, *17* (4), 247–261. https://doi.org/10.1631/jzus.B1500219.

(15) Jiang, H. S.; Zhang, Y.; Lu, Z. W.; Lebrun, R.; Gontero, B.; Li, W. Interaction between Silver Nanoparticles and Two Dehydrogenases: Role of Thiol Groups. *Small* **2019**, *15* (27), 1900860. https://doi.org/10.1002/smll.201900860.

(16) Flores-López, L. Z.; Espinoza-Gómez, H.; Somanathan, R. Silver Nanoparticles: Electron Transfer, Reactive Oxygen Species, Oxidative Stress, Beneficial and Toxicological Effects. Mini Review: AGNP BENEFICIAL AND TOXICOLOGICAL EFFECTS. *J. Appl. Toxicol.* **2019**, *39* (1), 16–26. https://doi.org/10.1002/jat.3654.

(17) Ferreira, E.; Giménez, R.; Cañas, M. A.; Aguilera, L.; Aguilar, J.; Badia, J.; Baldomà, L. Glyceraldehyde-3-Phosphate Dehydrogenase Is Required for Efficient Repair of Cytotoxic DNA Lesions in Escherichia Coli. *Int. J. Biochem. Cell Biol.* **2015**, *60*, 202–212. https://doi.org/10.1016/j.biocel.2015.01.008.

(18) Hoseini-Alfatemi, S. M.; Fallah, F.; Armin, S.; Hafizi, M.; Karimi, A.; Kalanaky, S. Evaluation of Blood and Liver Cytotoxicity and Apoptosis-Necrosis Induced by Nanochelating Based Silver

2022 S.T. Yau High School Science Award 仅用于2022年度丘成桐中学生科学奖公示

Nanoparticles in Mouse Model. *Iran. J. Pharm. Res.* **2020**, No. Online First. https://doi.org/10.22037/ijpr.2020.1101026.
(19) Gulati, S.; Sachdeva, M.; Bhasin, K. K. Capping Agents in Nanoparticle Synthesis: Surfactant and Solvent System; Bikaner, India, 2018; p 030214. https://doi.org/10.1063/1.5032549.
(20) Rather, R. A.; Sarwara, R. K.; Das, N.; Pal, B. Impact of Reducing and Capping Agents on Carbohydrates for the Growth of Ag and Cu Nanostructures and Their Antibacterial Activities. *Particuology* **2019**, *43*, 219–226. https://doi.org/10.1016/j.partic.2018.01.004.
(21) Balavandy, S. K.; Shameli, K.; Abidin, Z. Z. Rapid and Green Synthesis of Silver Nanoparticles via Sodium Alginate Media. *Int J Electrochem Sci* **2015**, *10*, 12.
(22) Nasrollahzadeh, M.; Sajjadi, M.; Iravani, S.; Varma, R. S. Trimetallic Nanoparticles: Greener Synthesis and Their Applications. *Nanomaterials* **2020**, *10* (9), 1784. https://doi.org/10.3390/nano10091784.
(23) Pacioni, N. L.; Filippenko, V.; Presseau, N.; Scaiano, J. C. Oxidation of Copper Nanoparticles in Water: Mechanistic Insights Revealed by Oxygen Uptake and Spectroscopic Methods. *Dalton Trans.* **2013**, *42* (16), 5832. https://doi.org/10.1039/c3dt32836h.
(24) Kanmani, P.; Rhim, J.-W. Physicochemical Properties of Gelatin/Silver Nanoparticle Antimicrobial Composite Films. *Food Chem.* **2014**, *148*, 162–169. https://doi.org/10.1016/j.foodchem.2013.10.047.
(25) Bearson, S.; Bearson, B.; Foster, J. W. Acid Stress Responses in Enterobacteria. *FEMS Microbiol. Lett.* **2006**, *147* (2), 173–180. https://doi.org/10.1111/j.1574-6968.1997.tb10238.x.
(26) Li, D.; Chen, S.; Zhang, K.; Gao, N.; Zhang, M.; Albasher, G.; Shi, J.; Wang, C. The Interaction of Ag2O Nanoparticles with Escherichia Coli: Inhibition–Sterilization Process. *Sci. Rep.* **2021**, *11* (1), 1703. https://doi.org/10.1038/s41598-021-81305-5.
(27) Moreno, M.; Hernández, R.; López, D. Crosslinking of Poly(Vinyl Alcohol) Using Functionalized Gold Nanoparticles. *Eur. Polym. J.* **2010**, *46* (11), 2099–2104. https://doi.org/10.1016/j.eurpolymj.2010.09.010.
(28) Gonçalves, A.; Castro, P.; Novais, A. Q.; Rangel, C. M.; Matos, H. Modeling of Catalytic Hydrogen Generation from Sodium Borohydride. In *Computer Aided Chemical Engineering*; Elsevier, 2008; Vol. 25, pp 757–762. https://doi.org/10.1016/S1570-7946(08)80132-0.
(29) Dai, L.; Nadeau, B.; An, X.; Cheng, D.; Long, Z.; Ni, Y. Silver Nanoparticles-Containing Dual-Function Hydrogels Based on a Guar Gum-Sodium Borohydride System. *Sci. Rep.* **2016**, *6* (1), 36497. https://doi.org/10.1038/srep36497.
(30) Upadhyay, L. S. B.; Verma, N. Synthesis and Characterization of Cysteine Functionalized Silver Nanoparticles for Biomolecule Immobilization. *Bioprocess Biosyst. Eng.* **2014**, *37* (11), 2139–2148. https://doi.org/10.1007/s00449-014-1191-8.

2022 S.-T. Yau High School Science Award
仅用于2022丘成桐中学科学奖公示